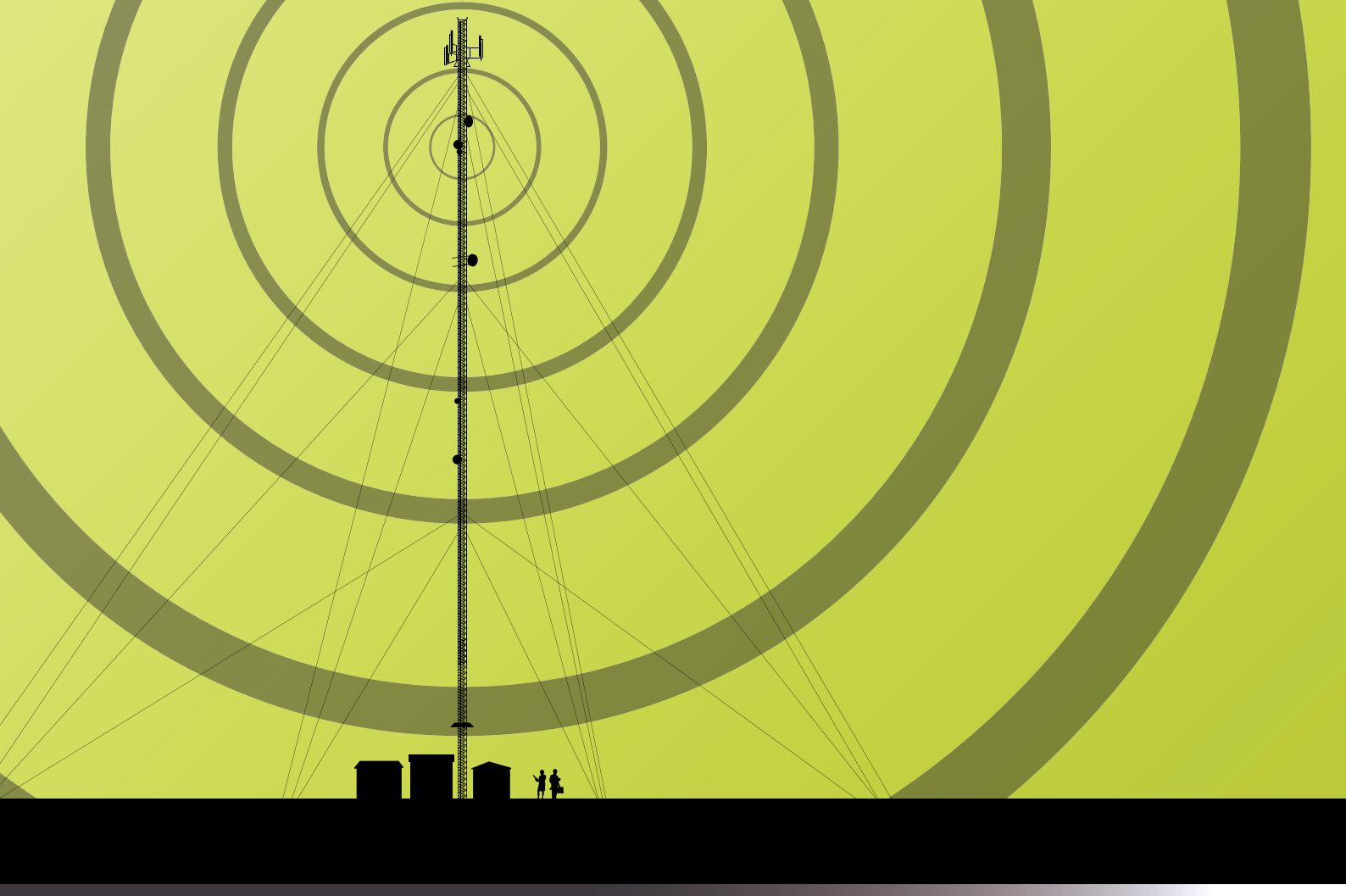

HANDBOOK ON GROUND WAVE PROPAGATION

EDITION OF 2014
RADIOCOMMUNICATION BUREAU

Handbook on

Ground Wave Propagation

Edition of 2014

Radiocommunication Bureau

Introduction

Ground wave propagation is of special interest for communication, particularly broadcasting, at the lower frequencies where the mode has been in use for more than 90 years.

The Handbook is divided into four main parts dealing with:

- the fundamentals and theory;
- the main, wide scale considerations and prediction methods used for compatibility assessments and planning procedures, used for spectrum management and coverage purposes;
- the smaller scale variability which may be of major importance in assessing the quality of services;
- measurements and phase.

Contributors to the Handbook, in alphabetical order, include:

Itziar ANGULO

Les BARCLAY

Yuri CHERNOV

Nick DEMINCO

Igor FERNÁNDEZ

Unai GIL

David GUERRA

John MILSOM

Iván PEÑA

David DE LA VEGA.

TABLE OF CONTENTS

Page

PART 1

Theoretical considerations

1 Introduction

At medium frequencies, during daylight hours, sky-wave signals propagating via the ionosphere are highly attenuated and the ground wave, or more strictly the surface wave, is the propagation mode which carries all signals which occupy the MF broadcasting band. Surface waves also support the operations of LF broadcasting, VLF/LF communication and navigation systems, HF short-range communication and some classes of HF radar – in these cases sky wave modes may also be present.

The surface wave propagation depends on currents which flow in the ground. The existence of the atmosphere changes the propagation characteristics but is not essential for the mode. Horizontally polarised surface waves are very heavily attenuated and have little or no practical worth. All the applications mentioned above utilise vertically polarised surface waves.

Unlike ionospherically propagated signals, the surface wave suffers negligible dispersion so that, in principle, wideband signals can be transmitted when the surface wave alone is active.

Fading only occurs when there is some temporal variation in the propagation path. Overland ground waves are stable signals, in some cases with some seasonal variation, and there may be variations over small distances where there are structures or significant topographic features. Over-sea surface wave propagation can be subject to slow fading due to changing tidal effects and attenuation due to sea roughness.

Methods based on the theoretical considerations, which form the basis of Recommendation ITU-R P.368, have proved over many years to provide a robust and rather simple way of predicting the coverage of, for example, MF and LF broadcasting systems. Methods for prediction in high-rise city areas remain incomplete. Additional losses due to local obstructions, severe topography, etc. are important, particularly when assessing the overall quality of a received service. Using robust modulation methods, time and frequency spreading of surface wave, and of combined surface and skywave modes, it is unlikely to cause significant degradation.

The first part of this Handbook introduces ground wave theory and goes on to describe techniques and prediction procedures suitable for overall wide-scale coverage predictions for spectrum management, planning and design purposes. However, particularly for systems with digital modulation, small scale effects due to buildings, topography, etc., may affect performance and service quality. Finally some information is given on measurements and on the relative phase of the ground wave.

2 The development of surface wave theory

In 1909 Sommerfeld [1] obtained a solution for a vertical electric dipole on the plane interface between an insulator and a conductor. Sommerfeld's work was not in a practical form for application by engineers and there was also an error which led to some confusion. In 1936 Norton [2] largely overcame these problems, and a further paper in 1937 [3] provided a method for calculations over a flat earth. Van der Pol and Bremmer [4] in a set of papers in 1937 to 1939 made it possible to calculate field strengths at distant points on the spherical Earth's surface, using a residue series. A further paper by Norton [5] in 1941 turned this into a more practical proposition for the engineer.

These methods still did not allow for variation of the Earth's constants (permittivity and conductivity) along the path. This is particularly important when the path is a mixture of land and sea, where the conductivities differ by a factor of about a thousand. In 1949 Millington [6] introduced a semi-empirical method to give fairly accurate results for a path which included changes in the Earth's constants. In 1952, Hufford [7] published a paper which allowed for arbitrary changes of both the Earth's constants and shape along the path. This is in the form of an integral equation which is, for all practical purposes, impossible to solve manually. In 1970 Ott and Berry [8] published a computer method for the solution of this equation.

In 1982 Hill [9] described an analytical method for extending the method of Ott and Berry [8] to propagation prediction over forested and built-up terrains that represents such terrains as dielectric slab layers over the irregular terrain. A source code appears in the Appendix of Hill's report. Further work published in 1986 by DeMinco [10], [11] provided user-friendly computer model implementations of the Ott and Berry [8] and the Hill [9] model. Also contained in these DeMinco models is a smooth spherical Earth mixed-path ground-wave model that uses Millington's method [6], [19], [20] for the mixed path computation described later, and also models for various LF, MF, and HF antennas for the purpose of system computations. The computer models have been verified using measured data by Kissick *et al*. [12], [13], Ott, Vogler, and Hufford [14], and Adams *et al.* [15]. Later work by DeMinco [16], [17] in 1999 and 2000 combined the smooth spherical Earth mixed-path model and the irregular-Earth mixed-path model with antenna models and system calculations into a Windows based LF/MF model [15], [17] for practical use as an analysis tool for point to point and area predictions with both ground-based and elevated antennas. Several sky-wave models were also included.

Rotheram [18], [19], [20] explored the influence of the Earth's atmosphere on surface wave propagation, and went on to develop a general-purpose ground-wave prediction method and an associated computer program. The method incorporates an exponential atmospheric refractivity profile and is the basis for the propagation curves for ground based antennas given in Recommendation ITU-R P.368.

The associated program, for the prediction of ground wave field strength for both grounded and elevated antennas over a spherical smooth earth, GRWAVE, is available on the ITU-R Study Group 3 webpage.

Early measurement campaigns of broadcast transmissions showed that there were anomalies in the propagation across city areas and Causebrook [21], [22] also showed that urban areas and irregular terrain cannot be described simply, because the current flowing in vertical conductors, and even in trees, effectively produces an inductive ground plane. This produces a very different attenuation with distance, compared to the simple smooth Earth, and the ratio of electric to magnetic field strengths is not equal to the intrinsic impedance of free space in this cluttered environment.

With the recent interest in digital modulation techniques there is renewed interest in small scale local variations in the signal, which for mobile reception correspond to temporal fading, since these may affect the quality of the received signal.

3 Surface wave Theory

3.1 Introduction to the theory

Consider the ease of a transmitting antenna, *T,* above a perfectly conducting flat ground as shown in Figure 1. The voltage, *V,* induced in the receiving antenna, at an arbitrary receiving position, *R* might be expressed as a vector sum of direct and ground-reflected components:

$$V = QI\left\{Q_1 \frac{\exp(-jkr_1)}{r_1} + Q_2 R \frac{\exp(-jkr_2)}{r_2}\right\} \tag{1}$$

where *I* is the current in the transmitting antenna, Q is a constant, Q_1 and Q_2 take account of the transmitting- and receiving-antenna polar diagrams, *R* is the appropriate reflection coefficient and *k* is the radio wave number = $2\pi/\lambda$. Other terms are defined in Figure 1.

FIGURE 1

Geometry of direct and ground reflected waves

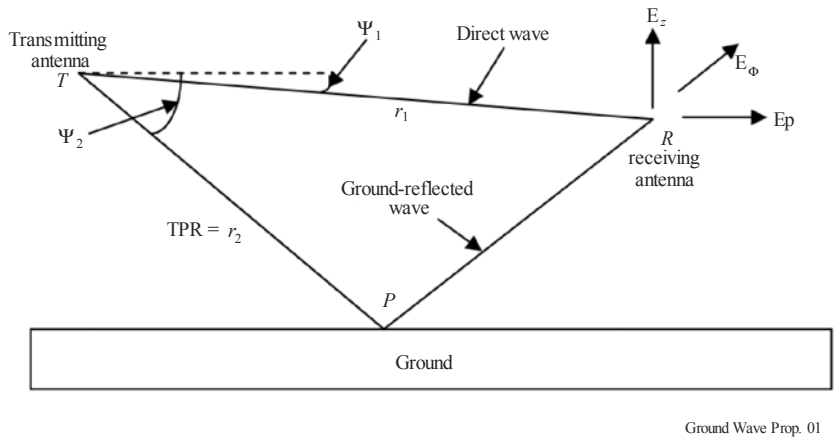

In many cases, especially where the radiated frequency is in the VHF or higher frequency bands, the above calculation will give a perfectly acceptable result for practical applications. However a complete description of the field at *R* requires an additional contribution to the resultant:

$$V = QI\left\{Q_1 \frac{\exp(-jkr_1)}{r_1} + Q_2 R \frac{\exp(-jkr_2)}{r_2} + S\frac{\exp(-jkr_2)}{r_2}\right\} \tag{2}$$

where *S* is a complicated factor which depends on the electrical properties of the ground, transmitted polarisation, frequency and the terminal locations.

When introduced in this way it is tempting to regard this as a minor contribution of interest primarily to the mathematical physicist. However, this third term represents the surface wave and it is a propagation mode of great practical value to radio systems operating in the HF and lower frequency bands.

Sometimes this combination of waves shown in equation (2) is called the ground wave, comprising a space wave and a surface wave:

$$ground\ \ wave = \underbrace{direct\ \ wave + reflected\ \ wave}_{space\ \ wave} + surface\ \ wave$$

But there are different uses of the terminology and the surface wave is often called the ground wave, or sometimes the Norton ground wave or Norton surface wave, after Norton who developed tractable methods for its calculation.

When the points *T* and *R* are close to the ground, the ground reflection coefficient is –1 and the direct and ground-reflected waves act to cancel each other, leaving the surface wave as the only important component.

3.2 Theory for a homogeneous smooth earth

3.2.1 Plane finitely conducting earth

Sommerfeld - Norton flat-earth theory:

Sommerfeld [1] and Norton [2], [3] derived expressions for the ground-wave field-strength components above a finitely conducting plane earth due to a short vertical current element. In its full form equation 2 becomes:

$$E_z = j30kIdl\left[\left\{\cos^2\psi_1\frac{\exp(-jkr_1)}{r_1}+\cos^2\psi_2 R_v\frac{\exp(-jkr_2)}{r_2}\right\}+\left\{(1-R_v)(1-u^2+u^4\cos^2\psi_2)F\frac{\exp(-jkr_2)}{r_2}\right\}\right] \tag{3}$$

$$E_\rho = -j30kIdl\left[\sin\psi_1\cos\psi_1\frac{\exp(-jkr_1)}{r_1}+\sin\psi_2\cos\psi_2 R_r\frac{\exp(-jkr_2)}{r_2}-\cos\psi_2(1-R_v)u\sqrt{(1-u^2\cos^2\psi_2)}\left\{1-\frac{u^2}{2}(1-u^2\cos^2\psi_2)+\frac{\sin^2\psi_2}{2}\right\}F\frac{\exp(-jkr_2)}{r_2}\right] \tag{4}$$

where ψ_1 and ψ_2 are defined in Figure 1, *Idl* is the product of source current and length (the 'dipole moment'), R_v is the plane-wave Fresnel reflection coefficient for vertical polarisation and F is an attenuation function which depends on ground type and path length. F is given by the expression:

$$F = \left[1 - j\sqrt{(\pi w)\exp(-w)}\left\{erfc\left(j\sqrt{w}\right)\right\}\right] \tag{5}$$

erfc denotes the complementary error function and

$$w = \frac{-j2kr_2u_2(1-u^2\cos^2\psi_2)}{(1-R_v)} \tag{6}$$

$$u^2 = \frac{2}{(\varepsilon_r - jx)} \tag{7}$$

and

$$x = \frac{\sigma}{(w\varepsilon_0)} = 1.8x10^4\frac{\sigma}{f_{MHz}} \tag{8}$$

σ is the conductivity of the earth in S/m, $\varepsilon_r = \varepsilon/\varepsilon_0$ is the relative permittivity of the earth and f_{MHz} is the frequency in MHz.

Note that equations (3) and (4) represent field components in the vertical and radial directions of a cylindrical co-ordinate system.

3.2.1.1 Special case of ground-based terminals

When the points T and R are both at the ground so that $R_v = -1$ and $\psi_1 = \psi_2 = 0$, the direct and ground-reflected waves act in opposition and sum to zero. Such circumstances will prevail in many practical applications at the lower frequencies. When this happens the surface wave dominates and may be described by somewhat simplified forms of equations (3) and (4), thus:

$$E_z = j60kIdl(1-u^2+u^4)F\frac{\exp(-jkr)}{r} \tag{9}$$

$$E_\rho = j30kIdl\left\{u\sqrt{(1-u^2)(2-u^2+u^4)}\right\}F\frac{\exp(-jkr)}{r} \tag{10}$$

Thus, for surface wave with ground-based antennas, the vertical and radial components of the electric field are still present. In physical terms this means that the propagating wavefront is tilted. The radial component given by equation (10) is small relative to the vertical component described by equation (9). The phase relationship is such that the modest wavefront tilt is forward in the direction of propagation. The degree of tilt depends on ground conductivity and frequency. Measurements of the wave tilt could be used to infer the electrical properties of the local ground (see section 18.3.3). Because E_ρ is finite and the magnetic field component is horizontal, there exists a downward component of the Poynting vector and energy is lost from the horizontally propagating wave. In this way attenuation occurs in addition to that due to ordinary inverse-square-law spreading. Within the Sommerfeld-Norton theory this extra attenuation is given by the term, *F,* see equation (5), where for ground-based terminals *w* simplifies to become:

$$w = \frac{-jkru^2}{2}(1-u^2) \tag{11}$$

3.2.1.2 Interpretation

Radio coverage predictions are almost invariably made in terms of electric field strengths. This also applies for LF and MF broadcasting even though most domestic receivers incorporate magnetic field antennas in the form of ferrite rods. Except for circumstances where a cluttered environment contains vertical conductors (see sections 11 and 12) the propagating surface wave contains a horizontal magnetic component, H_φ, which is approximately related to the major electric component *via* the expression:

$$H_\varphi = -\frac{E}{Z_0} \tag{12}$$

where Z_0 is the intrinsic impedance of free space (120π Ω). It is sufficient therefore to plan radio service coverages in terms of the electric field strength.

Attenuation of the surface wave arises through the forward tilt of its electric field. The rate of attenuation becomes more marked as the tilt angle increases. By combining equations (9) and (10), it is possible to show the ratio of electric field components to be simply related by:

$$\frac{E_\rho}{E_z} \approx u = \frac{1}{\sqrt{K_r}} \tag{13}$$

K_r is the complex dielectric permittivity of the ground. It varies with frequency and the electrical properties of the ground.

Some representative values are given in Table 1.

TABLE 1

Typical values of K_r, the complex dielectric permittivity, for different ground types and frequencies

Ground type	Frequency (kHz)	
	200 (LF)	**1 000 (MF)**
Sea (σ=5 S/m, ε_r=70)	70-*j*450000	70-*j*90000
Good ground ($\sigma=10^{-2}$ S/m, ε_r=10)	10-*j*900	10-*j*180
Poor ground ($\sigma=10^{-3}$ S/m, ε_r=4)	4-*j*90	4-*j*18

Large values of K_r correspond to a small forward tilt and therefore low attenuation. Sea water has an outstandingly high conductivity and the surface wave, with a near-vertical electric field, propagates over it with relatively low attenuation. On the other hand, surface-wave attenuation is greatest over ground of low conductivity and at high radio frequencies.

The factor $(1 - u^2 + u^4)$ in equation (9) is close to unity for all practical situations. It may then be shown that the amplitude of the vertical component of electric field is given by:

$$|E_z| = \frac{300}{r}\sqrt{P}|F| \tag{14}$$

where P is the total radiated power from a Hertzian-dipole current element, or from a short vertical radiator, expressed in kW, r is the path length in km and E is the electric field strength in mV/m.

This equation applies to a short vertical antenna located on a plane perfectly conducting ground and provides a reference.

Within a few wavelengths of the antenna $|F|$ is approximately unity and the field strength varies as 1/r, i.e. in an inverse-distance relationship. At sufficiently large distances, as long as the Sommerfeld assumption of a plane earth remains valid, $|F|$ makes a transition to become inversely proportional to distance; i.e. the field strength varies as $1/r^2$.

For a λ/4 vertical antenna the constant on the right-hand side of equation (14) becomes 314 (see Recommendation ITU-R P.341, Annex 1, Table 1, where this constant is listed as the cymomotive force).

Figure 2 gives the corresponding constant values for grounded vertical antennas of varying heights.

FIGURE 2

Cymomotive force for vertical antennas over perfectly conducting plane ground

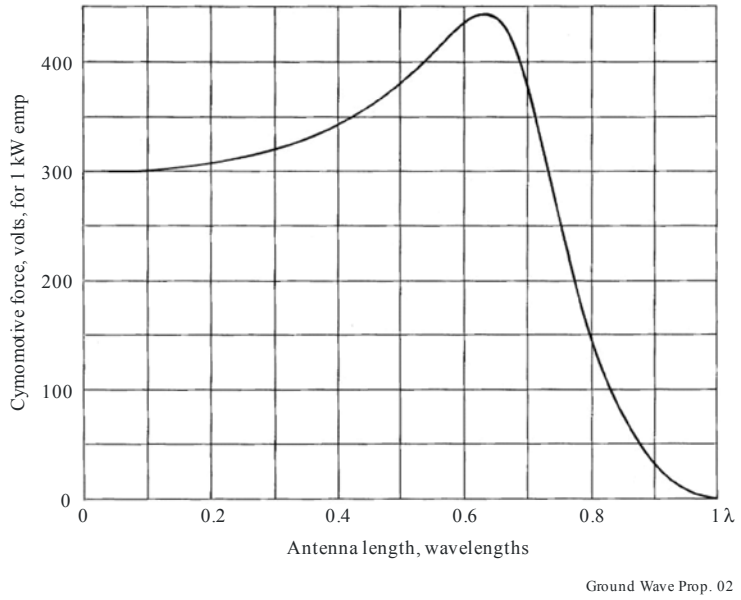

3.2.2 Spherical finitely conducting earth

The mathematics of ground wave propagation around the curved Earth is complicated and difficult to understand. It has been described by Bremmer [23]. At short ranges Sommerfeld's ground-wave model applies without adaption. At longer ranges it is necessary to compute fields with proper regard for diffraction around the curved earth. There is a third range regime, normally beyond that where inverse-square-law field variation occurs, in which the decrease in field strength becomes exponential around the curved earth. The starting distance of this exponential behaviour may be estimated by the expression below. The Earth can be considered flat out a distance *d* in kilometres given by [24]:

$$d = \frac{80}{\sqrt[3]{\mathrm{f(MHz)}}} \tag{15}$$

Apart from this additional far-range behaviour, most of the other characteristics of the surface wave above a spherical earth are identical to those deduced from Sommerfeld's plane earth model.

3.3 The effect of the atmosphere

The theoretical work of Sommerfeld, Norton, Van der Pol and Bremmer ignored atmospheric effects, assuming that a wave propagating in space above the ground would travel in a straight line. In practice, the Earth's atmosphere is stratified and possesses a refractive index which normally decreases with height. On average the height variation of refractive index is exponential. (see Recommendation ITU-R P.453).

In any atmosphere where the refractive index decreases with height, a radio-wave will be refracted downwards towards the ground. In the first kilometre above ground the exponential variation may be approximated as a linear decrease, and in this case radio paths may be treated as travelling in straight lines by artificially increasing the effective Earth radius. This treatment is often applied at VHF and higher frequencies [25] where a typical value for the effective earth radius factor is 4/3.

For surface waves at frequencies below 10 kHz the atmosphere has negligible effect and the factor tends to unity [26]. In the neighbourhood of the MF broadcasting band the factor lies in the range 1.20-1.25 for most classes of ground, see Rotheram [18].

These results are for typical atmospheric conditions (where the sea level refractivity is $N_o = 315$ and the scale height is 7.35 km) and are used in the graphical presentations in Recommendation ITU-R P.368. During times of non-typical atmospheric conditions, other effective earth radius factors may be required to simulate the prevailing propagation effects. Information on the atmospheric conditions may be available from local climatic observations or from Recommendation ITU-R P.453 and these parameters may be used as inputs in the computer program GRWAVE.

PART 2

The ITU-R recommended prediction method

4 Recommendation ITU-R P.368

The ITU-R recommended propagation curves for the field strength of the ground wave are given in Recommendation ITU-R P.368, based on the principles described in the section 3, above, calculated using the GRWAVE computer program. Although the method applies strictly for a smooth earth, satisfactory predictions will be obtained for ground with height irregularities which are small when compared with the wavelength, and where height changes are not abrupt. The variability due to small scale surface features, which may affect the quality of service, is discussed later in this Handbook. References [10], [11] demonstrate comparisons of predictions with measured data to show how the smooth spherical Earth computation compares with the irregular Earth computation. This information can be used to determine when it is necessary to use the irregular Earth model instead of the smooth Earth model. When possible, it is desirable to use the smooth-Earth model due to the excessive computation time when running the irregular-Earth mixed-path model even when using the high-speed computers that are available today. The issue of terrain resolution is also addressed in these references for computation accuracy over irregular terrain at LF and MF frequencies.

FIGURE 3

Example of the curves given in Recommendation ITU-R P.368

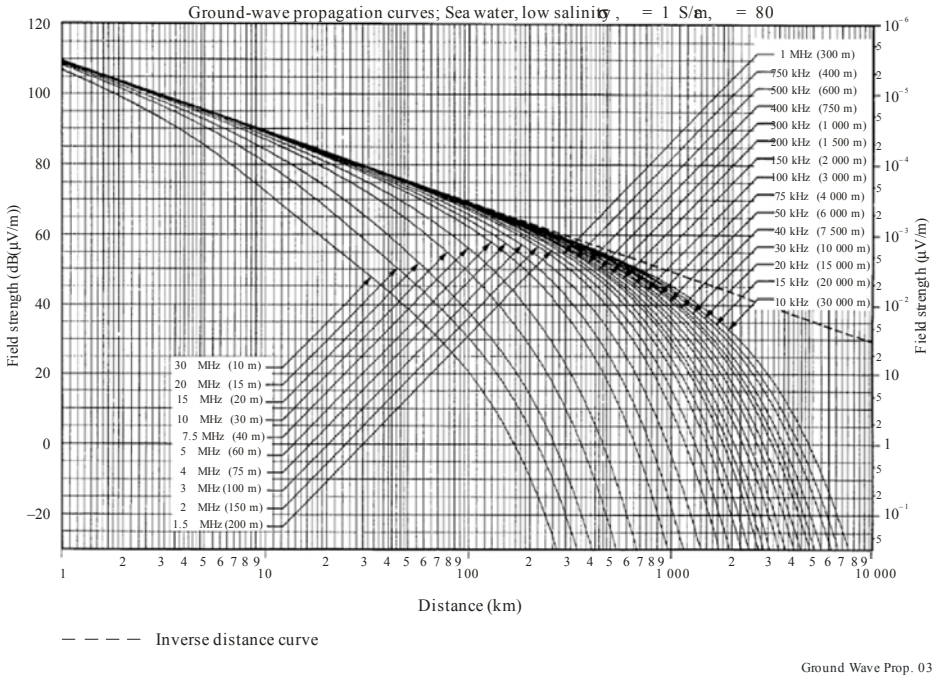

Propagation curves for higher frequencies are given in the ITU-R Handbook "Curves for radiowave propagation over the surface of the Earth", and various Recommendations deal with specific aspects of propagation at these higher frequencies (see Recommendation ITU-R P.1144).

Although the ground-wave curves are for antennas on the ground, the curves may be used for elevated antennas when $\varepsilon_r << 60\sigma\lambda$ for heights up to $h = 1.2\sigma^{1/2}\lambda^{3/2}$.

There are two sets of curves in the Recommendation. The first set has curves for frequencies between 10 kHz and 30 MHz where each figure is for a different value of the ground constants (the ground constants used are listed in Table 2). An example of one of these curves is given in Figure 3. For convenience, an alternative arrangement is also given in a second set of curves, where each figure is for a single frequency (from 30 kHz to 3 000 kHz) and for a range of ground constants.

TABLE 2

Graphs of ground wave propagation for various values of ground constants, given in Recommendation ITU-R P.368

Figure number	Description	Conductivity (S/m)	Relative permittivity
1	Sea water, low salinity	1	80
2	Sea water, average salinity	5	80
3	Fresh water	3×10^{-3}	80
4	Land	3×10^{-2}	40
5	Wet ground	1×10^{-2}	30
6	Land	3×10^{-3}	22
7	Medium dry ground	1×10^{-3}	15
8	Dry ground	3×10^{-4}	7
9	Very dry ground	1×10^{-4}	3
10	Fresh water ice, -1 °C	3×10^{-5}	3
11	Fresh water ice, -10 °C	1×10^{-5}	3

Each set of curves also includes the inverse distance curve as a dashed straight line.

For practical convenience, the curves are given for the case of 1 kW emrp; i.e. for 1 kW radiated omni-directionally from a short vertical radiator located on a smooth spherical earth. Allowance would need to be made for the actual or proposed transmitter power, for the losses in the coupling network feeding the antenna, for the azimuthal radiation pattern if directional antenna systems are used, and for the length of the antenna elements (Figure 2 gives the gain variation with antenna height in terms of the cymomotive force; Recommendation ITU-R P.341 also gives the gain for some reference antennas). Allowance would also need to be made for inefficiencies in the ground radial system of the antenna. A method of measuring the actual emrp of an existing system is described in section 18.2.

The program GRWAVE is also written for the same case of 1 kW radiated omni-directionally from a short vertical radiator located on a smooth spherical earth. To achieve this, the dipole moment used for the calculations is $5\lambda/2\pi$.

Note that the use of the transmission loss concept may lead to confusion where the presence of the ground restricts radiation to the half-space above the ground (see Recommendation ITU-R P.341, Annex 2).

The curves give the total field at distance r, with an error less than 1 dB when kr is greater than about 10, where $k = 2\pi/\lambda$. Near field effects can be included by increasing the field strength in decibels by:

$$10 \log \left\{ 1 - \frac{1}{(kr)^2} + \frac{1}{(kr)^4} \right\} \tag{16}$$

This gives the total field within ±0.1 dB for sea and wet ground, and within ±1 dB for any ground conductivity greater than 10^{-3} S/m.

An interesting discussion of the accuracy of determining the near field to far field transition boundary in terms of the minimizing the phase difference of the electric field across the aperture of either antenna, the amplitude error of the field strength prediction, and the distance necessary to make the $1/r^2$ and the $1/r^3$ terms of the electric field either significant (near field) or negligible (far field) in comparison to the 1/r field is contained in reference [27].

5 Surface impedance

An alternative way of considering the losses incurred with ground wave propagation is to start with the inverse-distance-squared relationship for signal power, (an inverse-distance relationship for field strength, as shown in Recommendation ITU-R P.368), and then to separately express the attenuation due to the losses of surface wave propagation.

The attenuation factor may be shown [28] to be:

$$A = 1 - i\sqrt{\pi\rho}\,\exp(-\rho)\,erfc\left(i\sqrt{\rho}\right) \tag{17}$$

and ρ may be expressed as

$$\rho = -\frac{i\pi\eta^2 r}{\lambda} \tag{18}$$

where η is the surface impedance given by

$$\eta = \frac{(\varepsilon - i60\sigma\lambda - 1)^{1/2}}{\varepsilon - i60\sigma\lambda} \tag{19}$$

The surface impedance is a useful way of describing complex surface features such as terrain irregularities, trees, man-made structures, buildings and sea waves.

6 Ground conductivity

6.1 The conductivity of land

For initial planning and for compatibility or frequency re-use assessments, the information in Recommendation ITU-R P.368, and its corresponding procedure in GRWAVE, is well established and widely used. However, the biggest uncertainty is likely to be in the estimation of the ground constants, and in particular of the ground conductivity. The electrical characteristics of the surface of the earth are discussed in Recommendation ITU-R P.527. It may be noted that the characteristics are expected to be independent of frequency at HF and lower frequencies (apart from the case of fresh water ice at LF and VLF.

However it is important to note the expected penetration depth, or skin depth, of radio waves into the ground[1]. For sea water the penetration depth (the depth at which signals are attenuated to 1/e of the surface value) is only about 25 cm at 1 MHz. But for medium dry ground it is about 25 m. Thus in determining or estimating the effective conductivity for use in predicting the coverage at MF, and even more at LF, it will be important to take proper account of the sub-surface geology. Further information on the depth of penetration of the electric field (skin depth) in soil and measurements of the dielectric properties of soil can be found in reference [68]**.**

Methods for determining the conductivity by using earth probes or other methods of measuring a soil sample are very unlikely to give useful results, since they will usually measure only the characteristics of the top soil. The most valid measurements would be made using test or operational transmitters and making a series of measurements at various distances, see section 18.3.

Recommendation ITU-R P.832 provides conductivity maps for both VLF and for MF. The VLF maps are for continental areas and extend over almost all of the land areas of the world. The MF maps are for many individual countries, or groups of countries, as provided by administrations. Opinion ITU-R 91-1 expresses the opinion that administrations should check and, if necessary, revise the information given in the World Atlas, noting that in some cases seasonal changes may need to be included; that new administrations should check that their needs are covered in the current World Atlas of Ground Conductivities and contribute to revisions of the data; and that for those countries for which no conductivity data are contained in the World Atlas, the administrations concerned should collect and provide data in accordance with the information given in Recommendation ITU-R P.832.

---

[1] The skin depth in an arbitrary material is given by:

$$\delta = \left(\frac{\sqrt{2}}{\omega \sqrt{\mu_r \mu_0 \varepsilon_r \varepsilon_0}} \right) \left[\sqrt{1 + \left(\frac{\sigma}{\omega \varepsilon_r \varepsilon_0} \right)^2} - 1 \right]^{-1/2} \tag{20}$$

where:

δ is the skin depth, $\omega = 2\pi f$, σ is the conductivity, μ_0 is the permeability of free space, μ_r is the relative permeability, ε_0 is the permittivity of free space and ε_r is the relative permittivity.

FIGURE 4

Example of ground conductivity map included in Recommendation ITU-R P.832

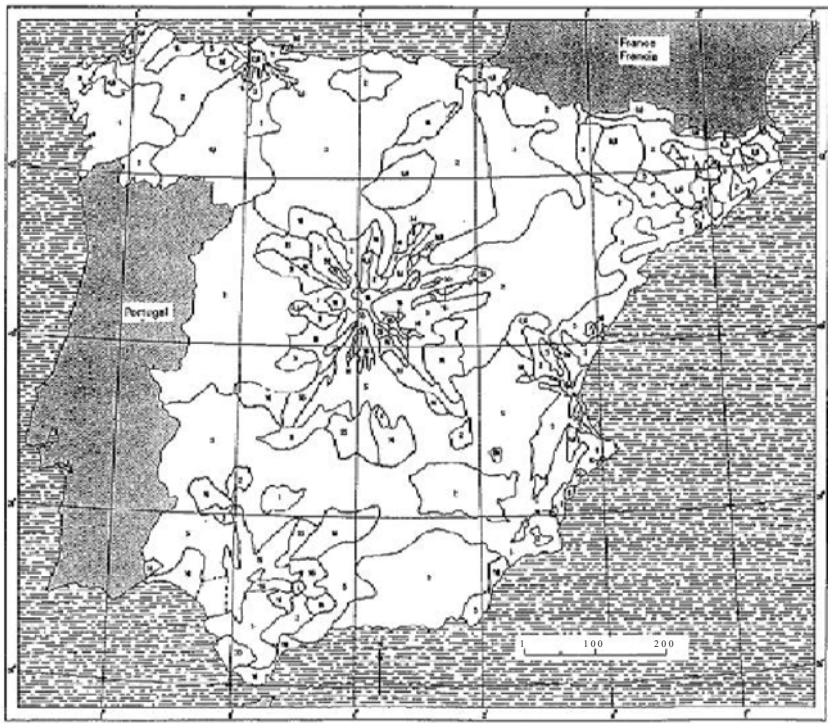

Ground Wave Prop. 04

Where there is no detailed information, a global map for conductivity at MF is also included in the Recommendation. However, this map only gives a broad indication of conductivity which may be adequate for global or regional assessments of spectrum requirements but is unlikely to be suitable for individual coverage estimation. Where no other information is available, the best way to estimate the conductivity is to examine geological maps and to compare the circumstances with another area of the world with similar geology and climate.

6.2 Sea conductivity

For sea water, Recommendation ITU-R P.368 provides predictions for typical and low conductivities of 5 and 1 S/m. The conductivity will however vary with both the salinity and temperature of the sea water, and for more precise predictions the expected conductivity may be used in the program GRWAVE.

The conductivity of sea water is given by:

$$\sigma = 0.18C^{0.93}\left(1 + 0.02\left(T - 20\right)\right) \quad \text{S/m} \tag{21}$$

where:

C: salinity (grams of salt per litre)

T: temperature (°C).

For cold seas, σ is of the order of 3.5 S/m and for warm seas is around 5 S/m.

PART 3

Variations from the main prediction procedure

7 Smooth earth of mixed conductivity

7.1 The over-sea recovery effect

Where the characteristics of the ground vary along the propagation path the resulting field strength has a surprising variation with distance. The field strength for a path extending across land, over sea and then over land again, decreases across the initial land region, but on reaching the coast recovers with a rapid increase followed by a more gradual decrease, and then a rapid decrease on crossing the coast again. Early methods of dealing with this problem gave incorrect results which did not satisfy the requirement for reciprocity. Millington [6] established a procedure which forced reciprocity and has proved to be very satisfactory for moderately smooth earth, giving results very similar to the more complex method developed by Hufford [7]. A theoretical study of propagation over a complex surface shows good agreement with the experimental results. [29]

FIGURE 5

The initial demonstration of the ground wave recovery effect over sea at 77 MHz

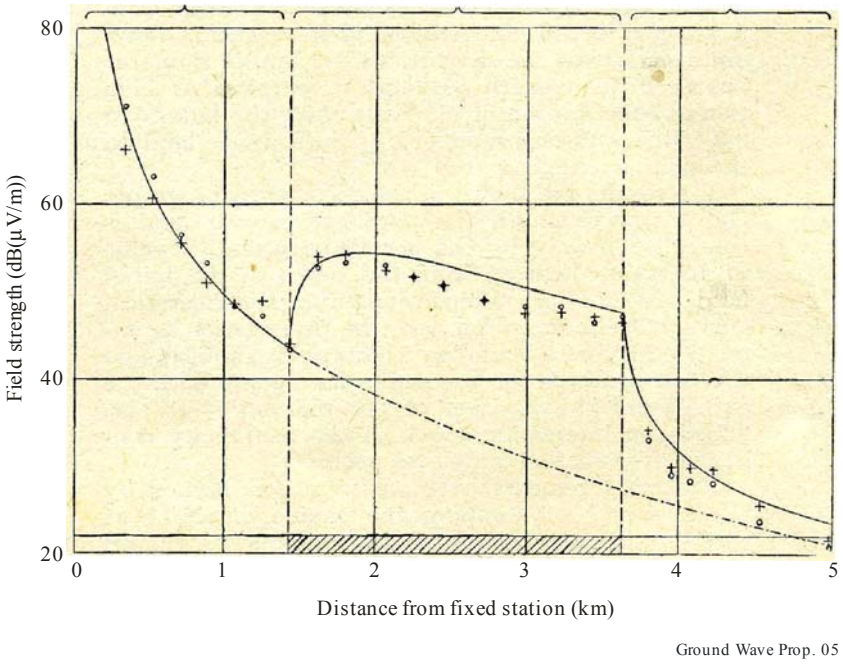

Millington's first tests were made at 77 MHz at short ranges and showed this recovery effect [30], see Figure 5. To confirm this effect, this initial test was followed by a long range experiment across the English Channel at 3 MHz [31], see Figure 6.

FIGURE 6

Tests of the ground wave recovery effect at 3 MHz

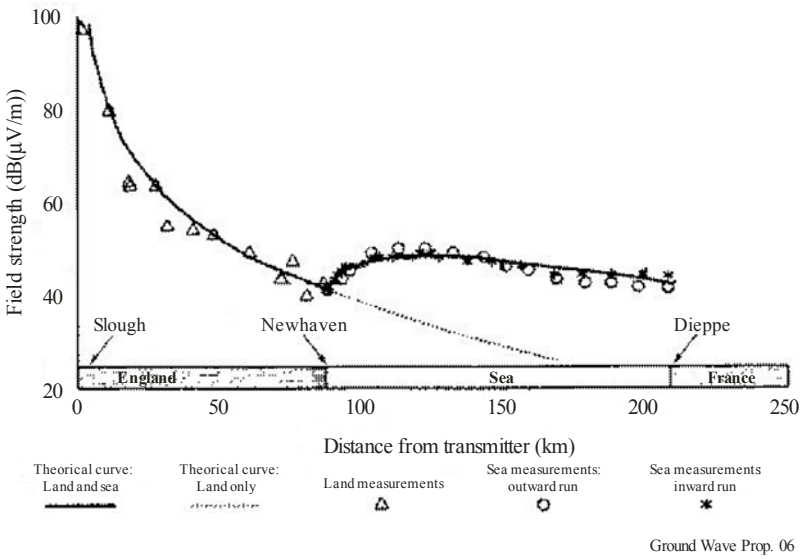

This effect is so unexpected that it may be necessary to demonstrate the effect again for new generations of engineers.

Other confirmations of the recovery effect are given in references [12], [14] which show the recovery effect over a land to sea path with good comparison agreement between propagation predictions and measurements for frequencies in the 100 to 2000 kHz frequency range. Reference [9] shows a similar recovery effect when a transition in the propagation path goes from a forest to an open field at a frequency of 10 MHz. Reference [32] shows the recovery effects over a land to water paths over measurements in the 285 to 325 kHz frequency range.

Figure 7 shows the result for a more complex test at 3.9 MHz on a land-sea-land-sea path in the Baltic Sea [33].

FIGURE 7

Tests of the ground wave recovery effect across the Baltic Sea

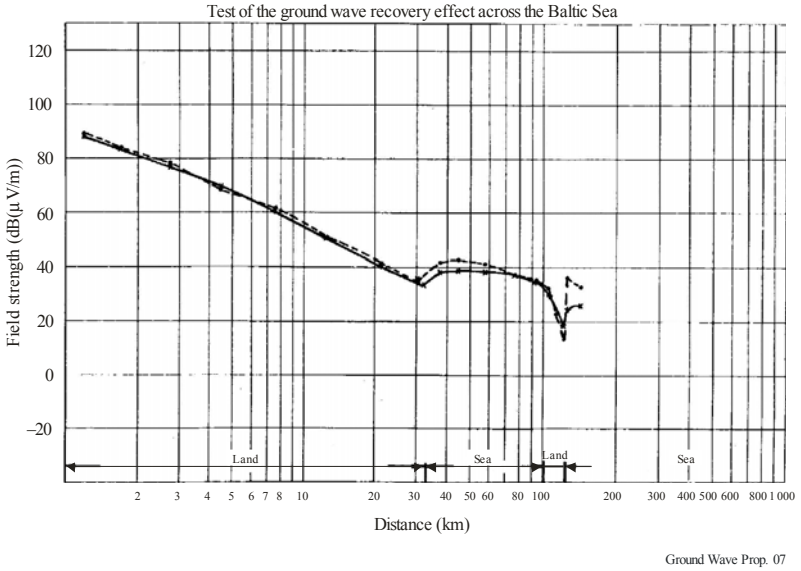

7.2 The Millington method for mixed paths

Millington's procedure, for example for a land-sea-land path, is to follow the ground wave field strength curve for the initial land section. At the coastal boundary the over sea curve is fitted to overland value at that location. The sea curve is then followed to the next coast and the appropriate overland curve is fitted at that range. The land curve is followed to the required distance. This gives the first intermediate value. The locations of transmitter and receiver are then interchanged and the procedure repeated for the reverse path to give a second intermediate value. The required prediction is then obtained by taking the geometric mean of the two intermediate field strength values (the arithmetic average when the field strengths are expressed in decibels).

This process can be undertaken with a simple graphical procedure if the curves are drawn with a linear distance scale or with a simple computer routine.

The procedure is also described in Recommendation ITU-R P.368 Annex 2:

Step 1. For a given frequency, the curve appropriate to the section S_1 is then chosen and the field $E_1(d_1)$ in dBμV/m at the distance L_1 is then noted. The curve for section S_2 is **then** used to find the fields $E_2(L_1)$ and $E_2(L_1+L_2)$ and, similarly with the curve for the section S_3, the fields $E_3(L_1+L_2)$ and $E_3(L_1+L_2+L_3)$ are found, and so on.

Step 2. The received field strength is then defined by:

$$E_R = E_1(L_1) - E_2(L_1) + E_2(L_1 + L_2) - E_3(L_1 + L_2) + E_3(L_1 + L_2 + L_3) \tag{22}$$

Step 3. The procedure is then reversed, and calling R the transmitter and T the receiver, a field E_T is obtained, given by:

$$E_T = E_3(L_3) - E_2(L_3) + E_2(L_3 + L_2) - E_1(L_3 + L_2) + E_1(L_3 + L_2 + L_1) \tag{23}$$

Step 4. The required field is given by the equation below:

$$E_M(R) = \frac{(E_R + E_T)}{2} (dB\mu V / m) \tag{24}$$

7.3 Estimation of a representative conductivity value for mixed paths at MF band

As indicated above the estimation of ground conductivity is likely to be most uncertain part of the prediction process, and where this applies it may not be justified to undertake the mixed path prediction procedure described above for overland paths where the varying conductivity is not too extreme. In these cases, a prediction method based on a representative conductivity value of the whole over-land part of a path can be used. References [32], [13] confirm this assumption for frequencies in the LF band near 300 kHz. References [12], [14] and [9] confirm this assumption for the LF and MF bands. Reference [1] supports this assumption for the HF band.

The weighted conductivity is defined as the average of the conductivity values along the path, weighted with the length of every conductivity section:

$$\sigma_{weighted}(mS/m) = \frac{\sum_i \sigma_i \cdot d_i}{\sum_i d_i} \tag{25}$$

where σ_i represents the different conductivity values along the path, and d_i represents the lengths of the sections along the path with a constant conductivity value.

The weighted conductivity is a representative conductivity value of the path that may be used in the prediction procedure. This provides good results for estimations of the field strength levels for all-land mixed paths. In the case of land-sea-land mixed paths, the weighted conductivity should be only used for the land sections, and then the Millington method should be applied.

8 Sea roughness

The effective conductivity of sea water is discussed in section 6 for smooth seas. However sea waves, causing surface roughness add additional losses, since energy is scattered out of the surface wave mode.

A widely used theory of HF ground-wave propagation over a rough sea is that developed by D.E. Barrick [34], [35]. This method is easily amalgamated with the smooth Earth ground-wave field strength method. Barrick has shown that the effects of a slightly rough surface can be modelled by replacing the smooth surface impedance by effective surface impedance which depends on the surface roughness. Barrick's theory is founded on three assumptions:

i) the surface height above a mean plane is small compared with a radio wavelength;

ii) the surface slopes are small;

iii) the medium below the surface is highly conducting.

These conditions are satisfied for HF propagation over the sea. They are violated for VHF radio waves over moderately disturbed seas and in either band in relation to propagation over land.

Examples of the sea state losses at 10 MHz are given in Figure 8, for the Phillip's model [36] of the sea wave spectrum. Generally, losses increase with path length, sea state and radio frequency. This figure shows a characteristic phenomenon: at distances up to 100 km from the coast, but beyond the range at which the recovery effect occurs, the field strength over slightly rough seas is greater than that over smooth seas. This is seen in Figure 8 for sea state 2. For a wavelength of 295 m an increase of 1.5 – 2 times has been observed [28].

FIGURE 8

Sea state losses at 10 MHz

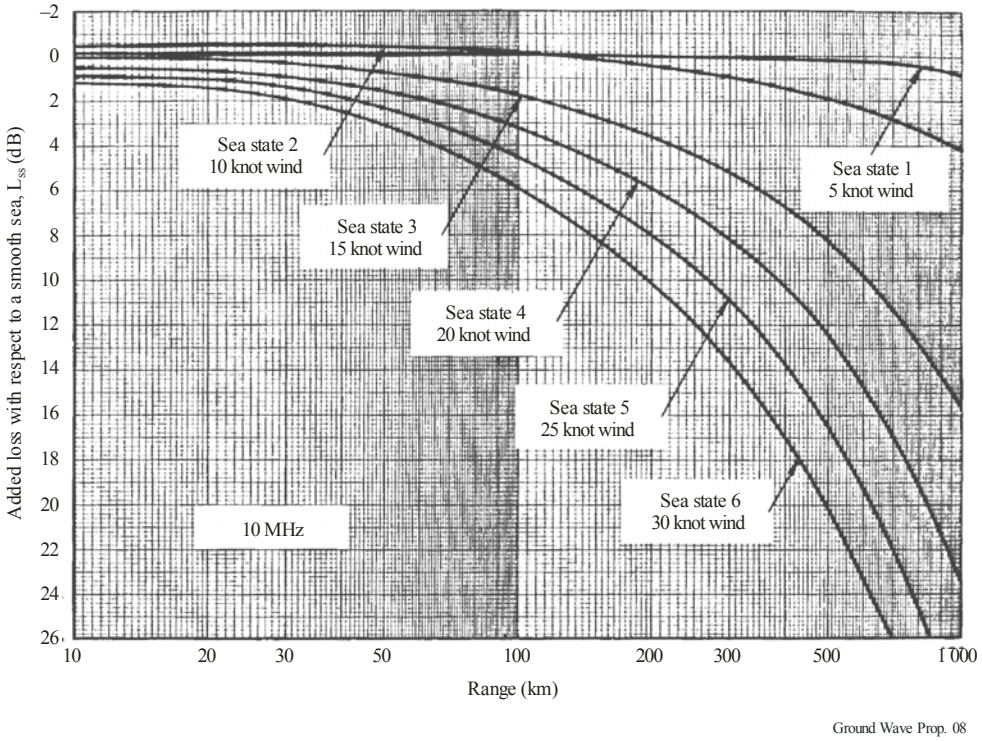

9 Rural environments

The mean field strength level in rural environment depends on ground electrical properties, frequency, distance to the transmitter and large scale variations due to the influence of the irregular terrain in the vicinity of the receiver location. All these aspects have been described in the previous chapters.

In practical situations in real environments, even where the distance between locations is much smaller than the distance to the transmitter, the reception conditions will not be identical due to the presence of local changes in the terrain, to trees and vegetation, buildings and man-made structures, overhead wires, etc. In many apparently open environments the difference in levels of a signal at nearby locations follows a log-normal distribution with a standard deviation averaging approximately 2-4 dB.

The special case of propagation across cliff edges was studied by Furutsu [37]. An example of the effect has been shown by Pielou [38].

10 Urban environments

10.1 The effect of the densely built up urban areas, 0.1 to 20 km

10.1.1 Introduction

There are a number of applications for which radio frequencies in the MF band may be used at short ranges (for example, the organization of urban and regional broadcasting networks, the development of utility services, etc.). It is thus necessary to know the characteristics of a field in the MF band at distances from several tens of metres up to tens of kilometres. However, the distribution and attenuation of medium frequencies in city regions, at distances shorter than a wavelength have been poorly studied.

Studies of the behaviour of the intensity in a city area of the electromagnetic far field have been studied, e.g. by Causebrook [22] (see section 10.2) and Chernov [39].

In the near field the field strength increases sharply at shorter ranges and that the rate of change for the electric and magnetic components is not the same. The component with the greatest increase depends on the type transmitter antenna. In particular, coming close to an electric field antenna (e.g. a vertical monopole), in the limit there is only the electric component caused by the current in the antenna.

At short distances the field decreases at first as R^{-3}, then as R^{-2} and in the far distance as R^{-1}. For urban building in these laws there are some peculiarities.

The initial assumption, as confirmed from preliminary studies, is that the attenuation of waves in areas with of urban buildings should be higher, than that for the smooth earth. If this excess is significant, the attenuation can be given in a simple formula.

10.1.2 **Brief theory** (see, for example [28], [60])

The field strength from an elementary electric radiator in a direction perpendicular to the axis of the radiator, for the electrical, $E_{el,}$ and magnetic, $H_{el,}$ components of the field

$$E_{el} = \left(\frac{iJklZ_0}{4\pi}\right)\left(\frac{\exp(ikR)}{R}\right)\left(1 + \frac{1}{ikR} - \frac{1}{k^2R^2}\right) \tag{26}$$

$$H_{el} = \left(\frac{iJkl}{4\pi}\right)\left(\frac{\exp(ikR)}{R}\right)\left(1 + \frac{1}{ikR}\right) \tag{27}$$

Similarly for a magnetic radiator the magnetic H_m and electrical E_m components may be written as:

$$E_m = \left(\frac{ikJl}{4\pi}\right)\left(\frac{\exp(-ikR)}{R}\right)\left(1 + \frac{1}{ikR}\right) \tag{28}$$

$$H_m = \left(\frac{1kJl}{4\pi Z_0}\right)\left(\frac{\exp(-ikR)}{R}\right)\left(1 + \frac{1}{ikR} - \left(\frac{1}{k^2R^2}\right)\right) \tag{29}$$

where J is the current in the radiator, l is radiator length, Z_0 is the wave resistance of free space ($120\pi\ \Omega$) and $k = 2\pi/\lambda$. The indexes "*el*" and "*m*" refer to the electric and magnetic radiators.

In the near field, where $R \approx 1/k$, exp (-*ikR*) can be approximated to unity so that:

$$E_{el} = JlZ_0 / (i4\pi R^3) \tag{30}$$

$$H_{el} = Jl / (4\pi R^2) \tag{31}$$

$$E_m = Jl / (4\pi R^2) \tag{32}$$

From these expressions it may be seen that the field strength close to the radiator increases sharply, and that the rate of increase for the electric and magnetic components is different. The ratio E_{el}/H_{el} in the near field increases in inverse proportion to the distance:

$$E_{el}/H_{el} = W / (iR) \tag{33}$$

From equations (26) to (29) it may be seen that, in the near field zone the field decreases as R^{-3}, then as R^{-2} and then, in the far zone, as R^{-1}. Also, in the near field the magnetic and electrical components are separated in phase by approximately 90 degrees, so that the field is reactive in character and is not radiated, as the Poynting vector is approximately equal to zero.

In many basic texts on electrodynamics and antennas (see, for example [40]) a complete analysis of a near field zone is not undertaken, and the way in which a distant field is created is not described. However, for the present purpose, an analysis of the near field is essential. For this purpose the term exp(-*ikR*) at short distances may be approximated as *(*1-*ikR),* and then equations (26) and (27) become:

$$E_{el} = \left(\frac{iJklZ_0}{4\pi R}\right)\left(-\frac{1}{\boldsymbol{k^2R^2}} - ikR\right) \tag{34}$$

$$H_{el} = \left(\frac{iJkl}{4\pi R}\right)\left(\frac{1}{ikR} - ikR\right) \tag{35}$$

From these expressions the modulus of the Poynting vector $\Pi = [H_{el}*E_{el}]$ consists of two parts. First, an imaginary part $\Pi_{im} \approx (kJl/4\pi)^2 Z_0/(k^3R^5)$; second, a real part given by the product of the real part of the magnetic component (where the first term in second brackets is obviously more significant than the second term) and the real part of the electric component. The magnetic component of the vector decreases as $1/R^2$, and the electrical component remains constant. Their product gives:

$$\Pi_{Re} \approx (k\mathrm{J}l/4\pi)^2 Z_0/R^2 \tag{36}$$

Thus near to the transmitting antenna the rate of decrease of power density is the same as in the distant zone, for which from (26) and (27) at large R we shall obtain (36). In other words, the real part of power density, radiated by an electric field antenna, varies with distance in the near, intermediate or distant zones as $1/R^2$ – corresponding to the usual law of spherical expansion. Characteristically, there is an increasing ratio of the imaginary to real components close to the radiator:

$$\Pi_{im}/\Pi_{Re} = 1/k^3R^3 \tag{37}$$

At MF the near zone is limited to distances much smaller than 1/k. Thus for wavelengths of 200 to 300 m where 1/k is 31 to 48 m the near zone is about 10 m.

In the distant zone, at MF beyond approximately 300-500 m, the intensity of a field is given by:

$$E = (300\ P^{1/2}/R)\cdot V \quad \text{mV/m} \tag{38}$$

where:

- P: radiated power in kW
- R: distance in km.

The attenuation function, V, depends on one parameter ρ:

$$\rho = -\mathrm{i}(\pi R/\lambda)\cdot[(\varepsilon'-1)/(\varepsilon')^2], \quad \varepsilon' = \varepsilon - \mathrm{i}\cdot 60\lambda\sigma \tag{39}$$

where:

- λ: wavelength in m
- ε′: complex dielectric permeability
- ε: real part of the permeability and
- σ: conductivity of ground in S/m.

For wavelengths in the range 200 – 300 m (1.5 – 1.0 MHz) and conductivities in the range σ from 10^{-3} up to 10^{-2} S/m:

$$\varepsilon' = \varepsilon - \mathrm{i}\cdot 60\cdot(\ 200\cdot 10^{-3}\ldots 300\cdot 10^{-2}) = \varepsilon - \mathrm{i}\cdot(12\ \ldots 180).$$

For low conductivity ground ε′, the first term in equation (39), can be neglected, so that:

$$\rho \approx 10^5\cdot\pi R/(6\lambda^2\cdot\sigma),$$

where R is in km, λ in m, σ in mS/m.

Accordingly, for σ = 1 mS/m and λ = 200 m, and for R = 1 and 10 km ρ = 1.31 and 13.1.

The attenuation function is approximately

$$V = (2 + 0.3\rho) / (2 + \rho + 0.6\rho^2) \tag{40}$$

For large values of ρ, equation (40) has a dependence close to 1/ρ, and the attenuation factor is proportional to R^{-1}.

Thus, for low ground conductivity and high working frequencies the dependence of field intensity with distance varies smoothly from 1/*R* (26) to $1/R^2$ at distances greater than approximately 1 km. At such distances, taking into account, (38) and (40) we have:

$$E = 300\, P^{1/2} \cdot 6\lambda^2\sigma /(10^5\pi R^2) = 5730 \cdot P^{1/2}\, \lambda^2\sigma/R^2 \qquad \mu V/m\ldots \tag{41}$$

where *P* in kW, *R* in km, λ in m, σ in mS/m.

It is important to note that $1/R^2$, as noted in [41], is theoretically the fastest rate of decrease of field intensity with distance from the transmitter in homogeneous urban conditions, at distances where it may be considered that the terrestrial surface is flat. The expression defines the limiting dependence, so that within the framework of the above assumptions, a more abrupt decrease with distance, in any conditions, would be expected to be impossible. Using this approach, a common solution, suitable for all distances, beginning from tens of metres is deduced by Chernov [41]:

$$E\,(R) = 74.72 – 33.36R – 10.47R^2 – 1.25R^3 + 367R^4 + 077R^5,\ \text{dB}\ (\mu V/m), \tag{42}$$

where $R = \lg (R, \text{km})$.

This dependence is shown in Figure 9.

FIGURE 9

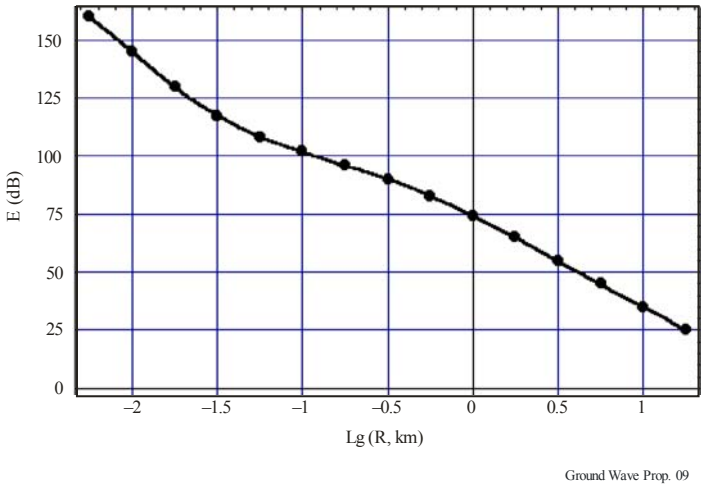

10.1.3 Results of measurements

To estimate the error of this curve (Figure 9) and to estimate the attenuation of MF signals at short distances from a transmitter, using a field strength meter with a shielded loop antenna, measurements on distances from the transmitter of up to 1 000 m in various urban conditions were undertaken [41], [61], [63].

The measured data of intensity of a field and theoretical dependence [41] are given on Figure 10.

FIGURE 10

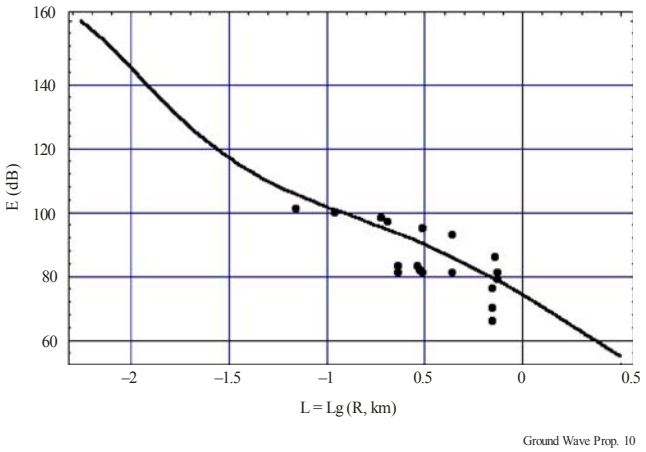

From the figure it may be seen that the measured data satisfactorily agree with the calculated curve. It is important to note that the experimental data are clustered together, not dropping out even when the measurements were carried out inside buildings. Exceptions occurred for measurements carried out in a lift, where the additional attenuation by metal walls was up to 40 dB.

These results together with those obtained earlier in a city at distances from 0.5 up to 30 km with a radiated power of 5 kW [41], are shown in Figure 11.

FIGURE 11

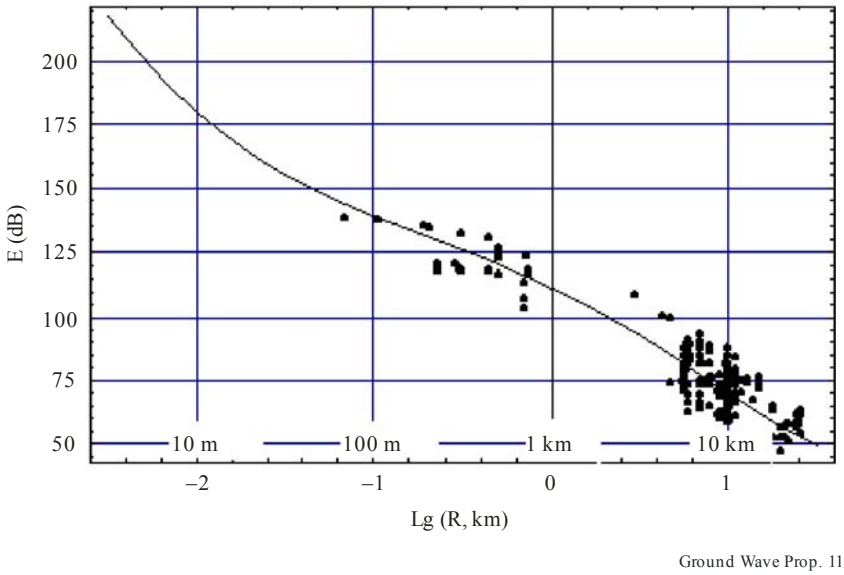

This research has shown, that at distances greater than 500 m, specific urban losses begin to have an effect, and MF propagation in urban built-up areas is similar to that for ground with poor conductivity, σ=1 mS/m.

Other series of measurements have been made of transmitters located in a city, with path lengths between 0.5 – 26 km on frequencies between 702 kHz and 1 539 kHz. Two examples of distribution of levels of a field along lines are given below.

So as to increase the quantity of data, Figure 12 groups the results of measurements of field strength for three transmitters, with frequencies near the bottom of the MF broadcasting band, and Figure 13 group results from four transmitters near to the top end of the band. The power of each transmitter is given as 5 kW.

In these two Figures the inverse-square-law curve is shown which fit the measurements rather well.

In addition to the above results for transmitters located within the city, research was also undertaken for suburban transmitters at distances from the transmitters from 10-12 km up to some tens of kilometers were carried out over a four day period. The field strength measurements were made with a moving measurement vehicle in the city of Moscow and the surrounding area. However, locations selected for analysis were limited to paths passing through the city centre (Figure 14).

FIGURE 12

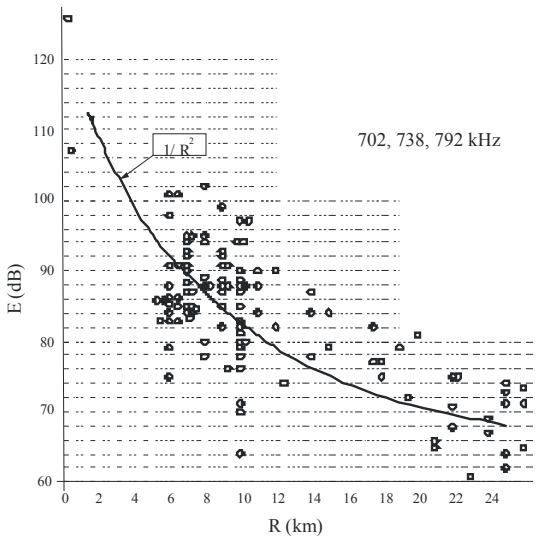

FIGURE 13

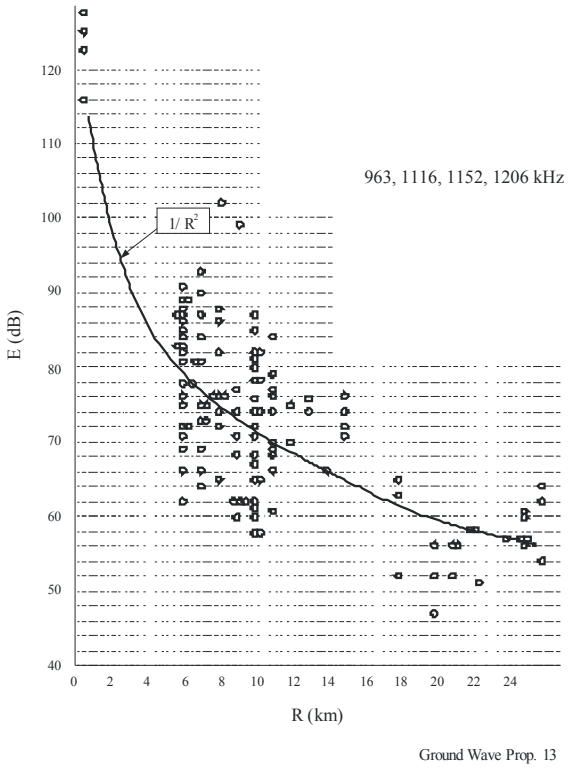

FIGURE 14

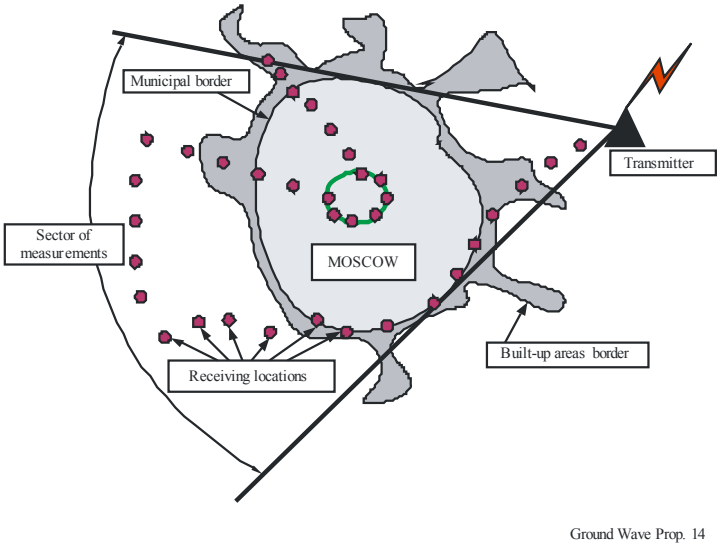

Figures 15 and 16 give examples of the results for one of the suburban transmitters on two different frequencies.

FIGURE 15

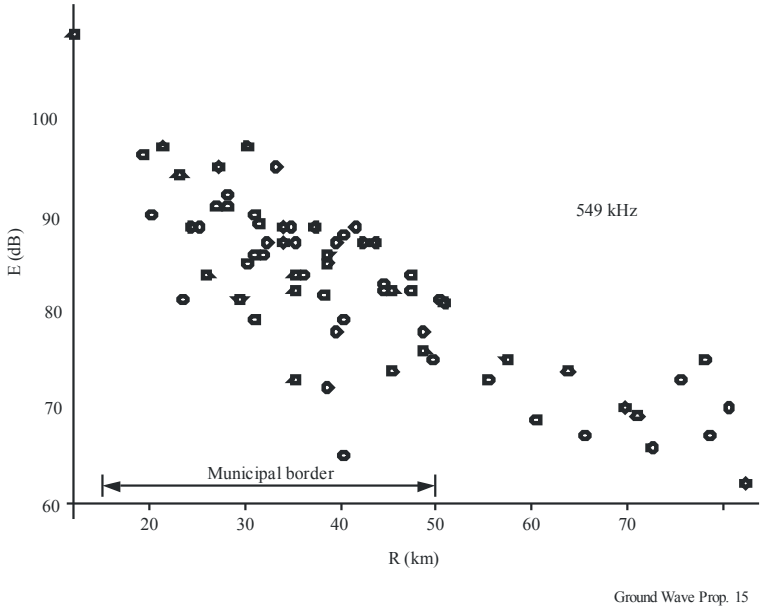

In addition to results obtained at medium frequencies, similar work [42] devoted to similar researches in a HF-band should be noted. This showed that at distances from the transmitter of up to 100-700 m the field strength is practically proportional $1/R$, whereas at distances of 0.7-10 km the law becomes rather close to $1/R^2$. Additional details of the measurements in the Moscow area given in [39].

FIGURE 16

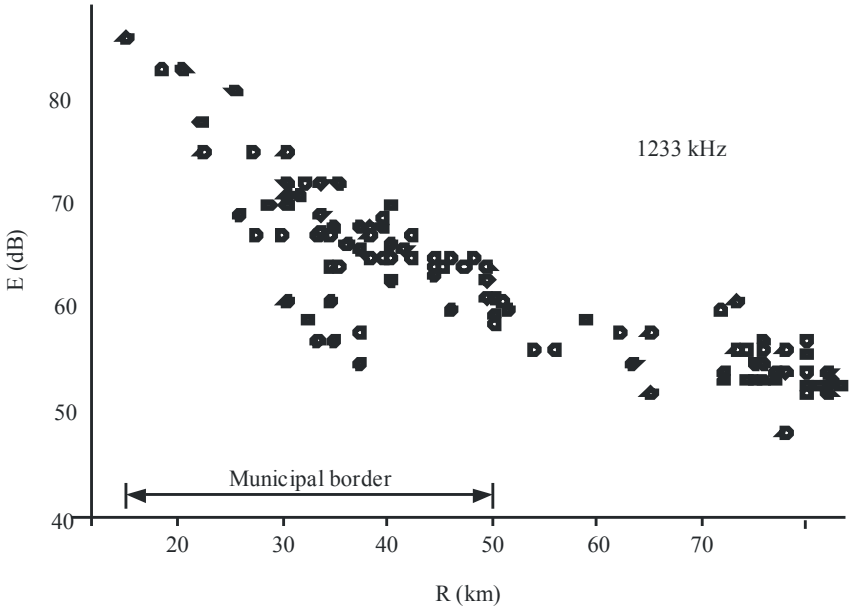

10.2 Distances beyond 25 km

Following the introduction of MF broadcasting in the 1920s, investigations were undertaken into the variations of the received signal. The effects of ground conductivity, terrain height and irregularities, screening by buildings, etc., the night time effects of the, as then unknown, ionospheric sky-wave and particularly the increased rate of attenuation with distance in city areas [43], [44], [45], [46] were noted. Once the general principles of MF ground wave propagation were understood, it turned out that overall coverage predictions based on smooth earth propagation of appropriate conductivities proved to be quite adequate in most cases for high power transmissions covering a mixture of rural and urban environments. However, a renewed interest in more local broadcasting aimed primarily at towns and cities and their suburbs showed the inadequacy of such methods in city areas. This will become of increasing importance for digital broadcasting, where there is a more critical boundary between satisfactory reception and failure at low signal/noise ratios.

The effect of buildings and other structures containing conducting vertical elements, and of trees, was identified by Bown *et al*. [44], who explained the effect in terms of resonant circuits in the vertical structures. Later Causebrook [47] made studies across London and developed an explanation for the effects observed in densely built-up areas. Measurements were made at three frequencies, on two azimuths across London; see Figure 17.

FIGURE 17

Measurement paths across London

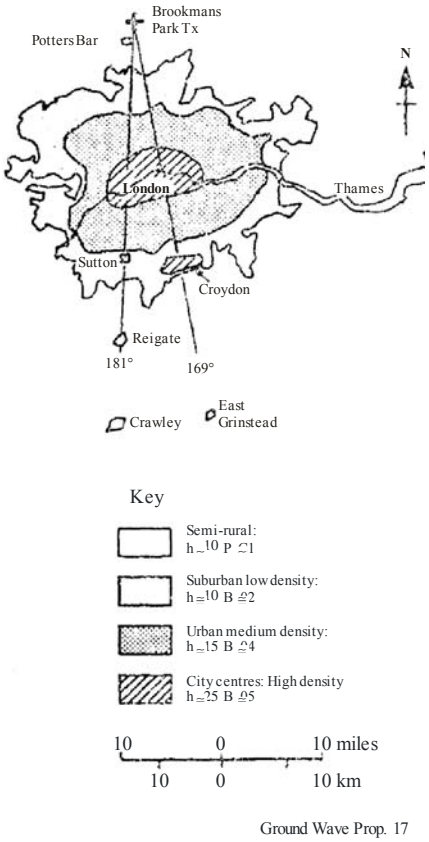

Ground Wave Prop. 17

Figure 18 shows Causebrook's measurements across London for the azimuth of 169 degrees. On all three frequencies the field strength near to the transmitter does not decrease in the expected way, but then there is a rapid decrease to a minimum followed by a recovery. He considered the modification of the surface impedance due to a structure like a bed of "conducting nails". He examined the complex plane of the function ρ (see equation (18)) and plotted the attenuation A (see equation (17)) and phase, as shown in Figure 19.

FIGURE 18

Measurements at three frequencies across London

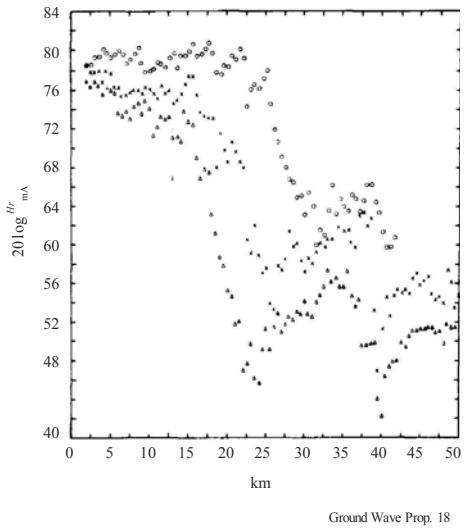

He showed that for smooth earth and for most rural environments, propagation lies in the bottom half of Figure 11, where the contours have a regular shape. However, results in the dense urban environment are in the upper half of the figure where there is an unusual attenuation variation, including a null point.

A calculation method was proposed where the path was segmented into parts with different conductivities and surface features, which included parameters for the height of man-made structures and for the fraction of the area covered by buildings. This method has, so far, not been developed nor widely tested as a prediction tool.

Another approach to this problem has been given by Luo [48]. This method defines a series of loss components for the path length, reflection, diffraction and refraction around buildings, etc.

FIGURE 19

The complex ρ plane

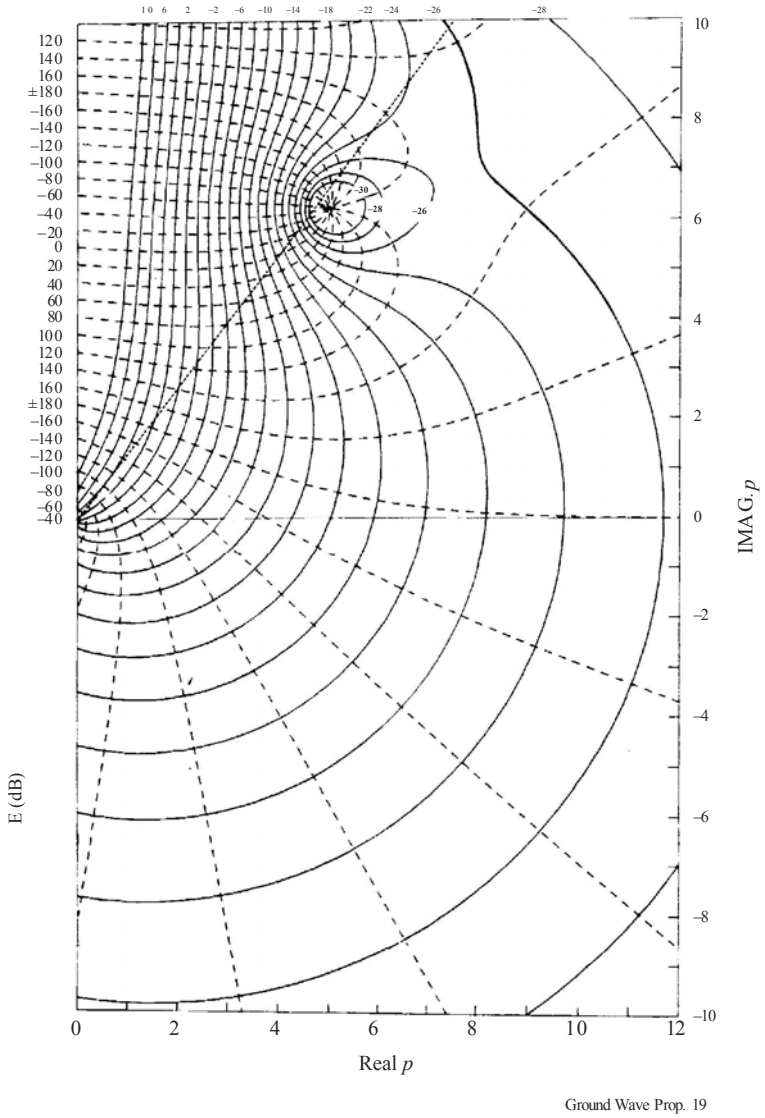

11 Seasonal variations in surface wave propagation

In some cases there may be seasonal variations in surface wave propagation. These may be due to changes in the refractivity of the troposphere (see section 3.3) or to the state of vegetative cover; to changes in the level of the water table within the ground; to freezing conditions where water becomes ice, or to thick snow-cover, etc., where these may cause changes in the effective ground conductivity. All of these changes may affect the intensity of the surface wave field. In particular such seasonal changes may result in a reduction in field strength in summer.

11.1 History

Measurements of the signal level in day time of an MF station near to Philadelphia, USA [49] were first made in the 1920s at ranges up to several hundred kilometers. Measurements showed that half-hour medians from day by day do not remain constant, but changed by up to several decibels. In addition, the average signal level also changed from month to month, with a seasonal variation, of greatest size in the winter months. The monthly average values of seasonal changes of a signal level were up to 4-5 dB. Attempts were made to determine the reason of such changes of the signal. Correlation of signal level changes with ambient

temperature, humidity, pressure and other atmospheric parameters were determined. The greatest value of negative correlation was found with temperature. The physical reasons of this phenomenon were not clear. An example of changes of signal level on an annual interval is given in Figure 20.

FIGURE 20

Example of seasonal variation recorded in USA

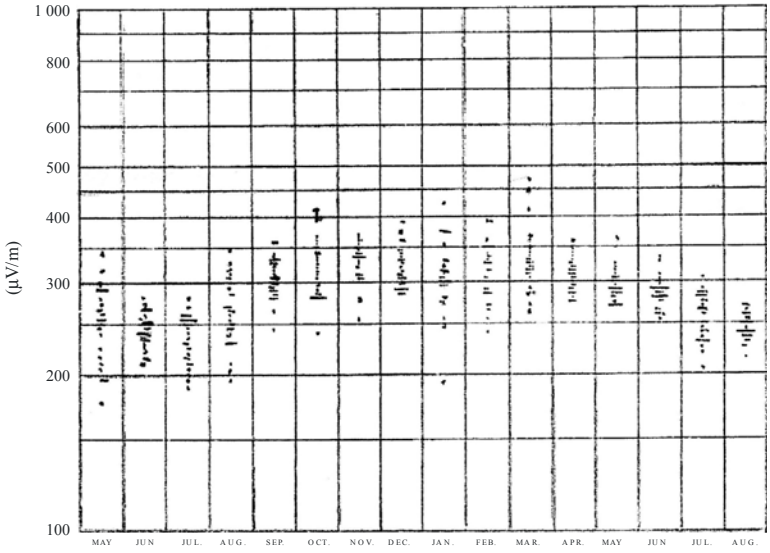

Daily 1:30 P.M., EST, field intensities, Philadelphia, Pa., (WCAU) to Baltimore, Md. 1 170 km, 76 miles. May, 1939-August, 1940.

Ground Wave Prop. 20

Similar measurements were carried out in Switzerland at MF, at ranges of up to 100 km during the years 1938-1944. The results were published in 1945 [50]. The mid European climate has a greater temperature range, and the seasonal changes also have a larger value, up to 8 dB. The results received in Switzerland in day time, are shown in Figure 21.

FIGURE 21

Example of seasonal variation recorded in Switzerland

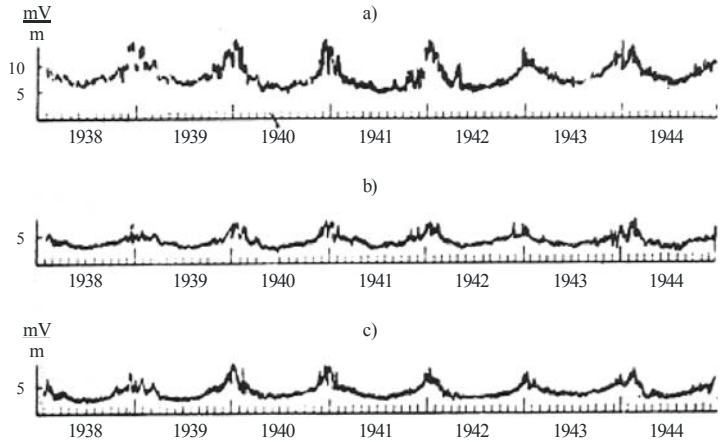

Ground Wave Prop. 21

At the end of the 20th century, measurements were made on many frequencies in the LF and MF bands at various time of day on paths of various extent, from 11 up to 2 500 km near to Moscow and in the Siberian Region.

The results of the first measurements in the Moscow area are given in [51]. In more complete and longer measurement programmes the values of seasonal changes at MF on various paths near to Moscow were on average 10-15 dB.

In the Siberian Region, where the greatest differences of temperatures occur from winter to summer, changes of approximately 15 dB and more are observed [52]. An example of changes of intensity of the field near to Tomsk is given in Figure 22. Paths located in middle latitudes with a significant part of a tree cover have the greatest seasonal changes of signal level, of 5-15 dB or more [53], [54]. Table 3 shows the average values of the change H (dB) between winter and summer months [61].

FIGURE 22

Seasonal variation of field strength at 576 kHz with temperature for a 155 km path near Tomsk

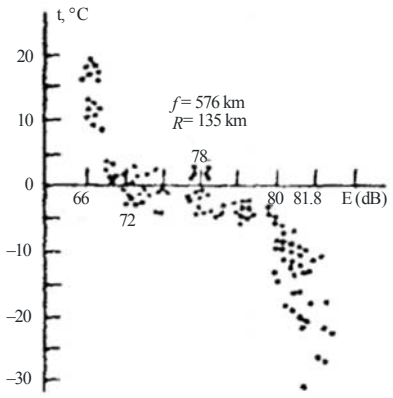

Ground Wave Prop. 22

TABLE 3

Seasonal variation in signal level

Average January temp (ºC)	4	0	–10	–16
Typical variation, H (dB)	4	8	13	15

The above results are reflected in Recommendations ITU-R P.368-9 and P.1321-3.

11.2 Day by day variations in surface wave propagation

Day to day changes are also observed on all MF paths in the Moscow region [39], and on the majority of LF paths. Examples are shown in Figure 23. The operating frequencies and path lengths are specified in the legend. At LF the rms deviation in signal level ranges from fractions of a decibel on short paths at the low-frequency edge of the band, averaging 0.8 dB, to approximately 10 dB in the higher-frequency part of the band for path lengths of up to 1 000 km and more. At MF changes of signal level for paths of tens of kilometres are much larger than at LF, typically 2-4 dB, and occasionally up to 5-6 dB, see Figure 24.

Fading on ground wave paths have a strong dependences on frequency and path length. In the MF band even paths of 20-100 km have rms variations with appreciable dependence on season and frequency, as seen in Figures 25 and 26.

FIGURE 23

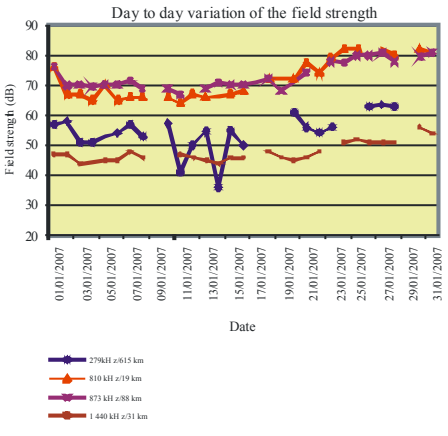

FIGURE 24

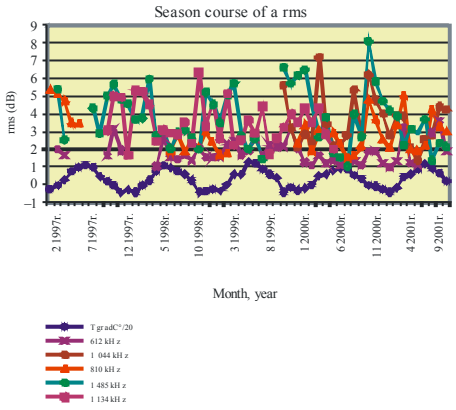

FIGURE 25

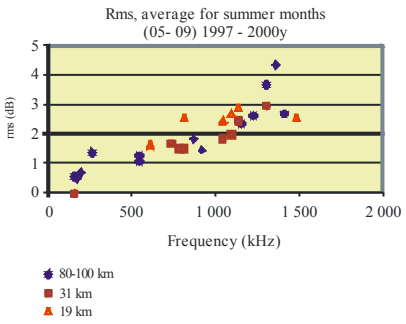

FIGURE 26

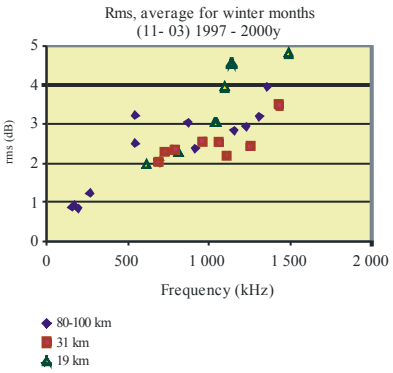

PART 4

12 Receiving antennas

As discussed in section 3.2.1.2, in open environments the vertical electric field strength and the horizontal magnetic field strength are related, according to equation (12). Antennas used for measurement and for service reception may be rod or wire antennas responding to the electric field (such as some car radio antennas), or loop of ferrite antennas responding to the magnetic field (such as in domestic broadcast receivers).

In obstructed environments the spatial variability of the electric field is often considerably greater than for magnetic antennas. Most portable field strength measuring receivers use loop antennas calibrated for the electric field using equation (12).

Figure 27 shows the variation for both the electric and magnetic field antennas on two example routes [55].

FIGURE 27

Measurements on two routes with magnetic and electric antennas

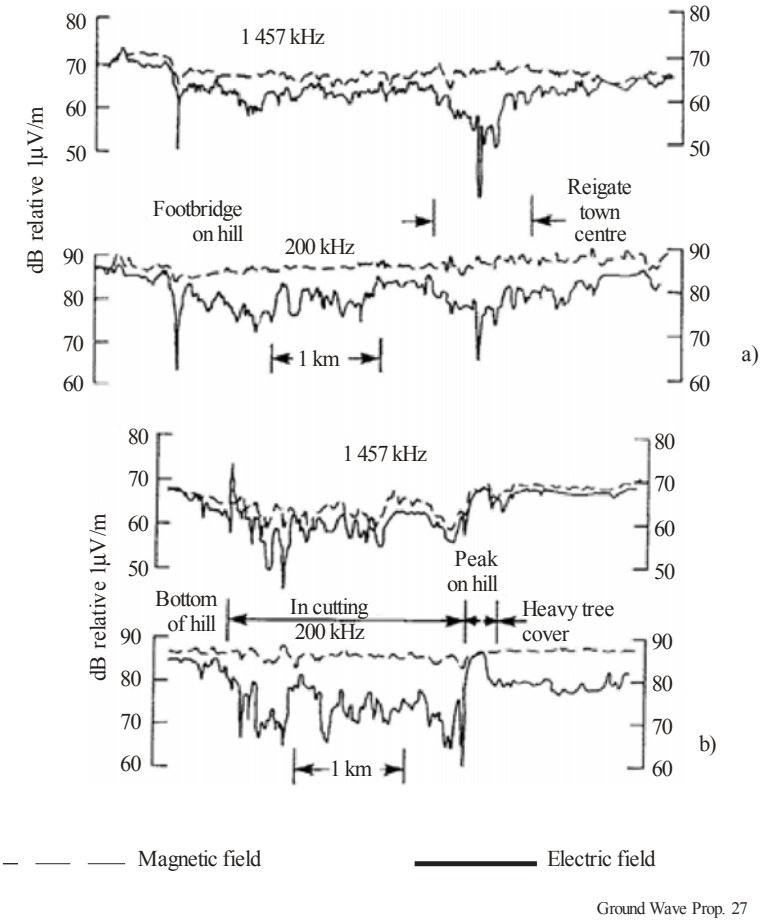

Ground Wave Prop. 27

13 Characterization of field strength spatial variability

The text above provides a characterisation of the general behaviour of the surface wave propagated across areas with various conductivity values and across sea and city areas. Due to local effects, changes in topography or the presence of individual structures or groups of structures, etc., the received field strength will vary within distances of a few metres.

The field strength variability can be expressed as the combination of two terms. Each of them represents a signal component of a different nature, whose variations are due to differentiated causes [56]:

– Large-scale spatial variability *m(x)*: is caused by large-scale variations along the path between transmitter and receiver. In the case of ground-wave propagation it is due to the alteration of transmitter-receiver path features or the urban reception environment and the influence of both the electrical characteristics of the terrain and the terrain roughness.

– Small scale spatial variability $r_0(x)$: represents the local variations of the signal, superimposed upon the large scale median level, mainly due to the influence of the local reception environment, such as the variations caused by different elements such as bridges, power lines, etc.

The relation between them, in linear scale, is:

$$r(x) = m(x) \cdot r_0(x) \tag{43}$$

The long-term component *m(x)*, or large-scale variability of the signal, is obtained by averaging the signal *r(x)* in order to remove the influence of the local environment where the receiver is located. The signal *m(x)* corresponds to a series of local mean values of the signal *r(x)* for mobile reception.

The short-term component $r_0(x)$, or fast signal variation around the mean value *m(x)*, represents the local variations of the signal *r(x)*. Thus, for estimating the short-term component, the long-term component must be previously calculated by averaging the signal samples located within an interval around each location, and then removing this component from the signal envelope.

A proper differentiation of the components *m(x)* and $r_0(x)$ of the signal allows a more accurate analysis of the spatial signal variability and a correct determination of the sources that cause the mean attenuation of the field strength in an extended area, and the local variations of the field strength due to the local reception conditions.

The Generalized Lee Method (see Annex 1) is the reference method for estimating the local mean values of the long-term signal along a route. Figure 28 shows an example of the instantaneous and the long-term spatial variation of a signal recorded whilst in motion in an urban environment. The short-term variation is the rapid variation around median local values.

FIGURE 28

Long-term spatial variation of field strength in urban reception

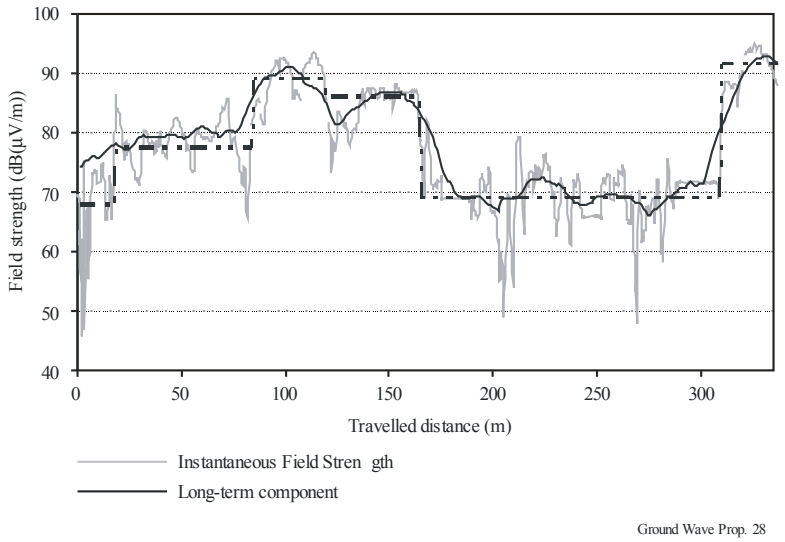

14 Irregular terrain

Although the ground electrical properties are the main factor that determines the attenuation of the surface wave, the roughness of the terrain generates additional path losses in the MF band [8], [57], [58]. These field strength losses are significant only when the transmitter-receiver path is obstructed by high terrain irregularities (compared to the wavelength) located near the receiver location. All significant irregularities along the entire length of the path have an appreciable effect on the total losses along the path even though the irregularities near the receiver can have a predominant effect, especially if the slope on the far side of the irregularity is steep [11]. The field strength level diminishes in those reception sites located behind such obstacles. This signal variation depends on the extent of the obstruction caused by the terrain irregularities along the path profile, and it can be estimated as an additional attenuation factor that should be added to the path transmission loss mean value.

FIGURE 29

Field strength variation as a function of the distance to the transmitter recorded in a measurement campaign. Terrain elevation values recorded by the GPS receiver are shown

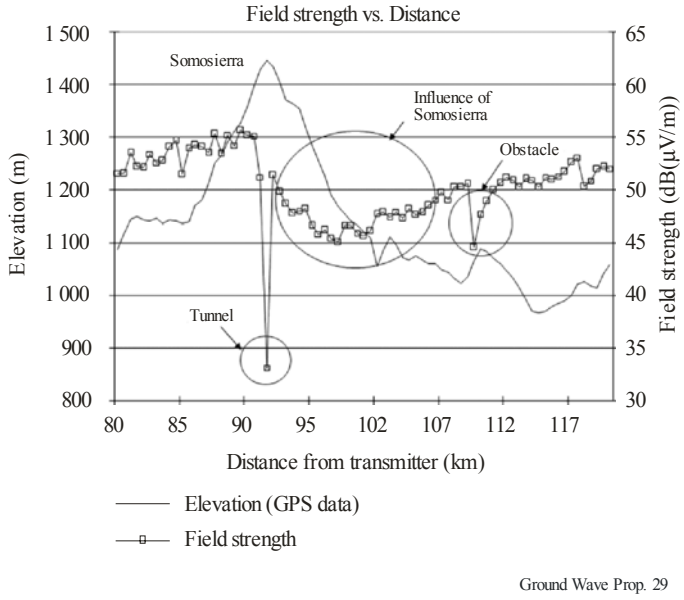

Figure 29 shows an example of the field strength variation when the receiver travels along a route, and the terrain irregularities obstruct the transmitter-receiver path. The route is virtually radial from the transmitter and it crosses the Somosierra mountain range (Spain). In the Figure, the measurement route values 12 km before and 28 km after the summit of Somosierra are depicted with their corresponding range height profiles. A tunnel goes through the mountain range near the summit, causing a deep fading in the field strength signal. A remarkable field strength attenuation can be observed at the "shadowed" side of the mountain (more than 10 dB if median values are considered).

At the shadow side of the obstacle, as the receiver moves away from the transmitter, the field strength values follow an upward trend. This behaviour of the field strength in the vicinity of the terrain irregularities, as a function of the distance to the transmitter, is explained by Ott [44], and previously predicted by Wait [59], as a constructive interference of a direct diffracted ray and a diffracted ray traveling along the surface.

Following the analysis of the example, the next field strength drop was measured at 109.5 km, and is due to a second lower obstacle, which is not very high ($\lambda/4$ height, where λ is 221 m) but is very close to the receiver location. The short distance from the obstacle to the receiver location appears to be a very influential parameter. The slope of the far side of the irregularity (toward the receiver) is a major determinant of the path losses, which would most likely occur for a short distance from the irregularity to the receiver.

The field strength attenuation due to the obstruction of a significant obstacle depends mainly on two parameters [67]:

– the distance d between the obstacle and the receiver location;

– the obstacle height h over the line-of-sight between transmitter and receiver.

At a specific obstructed receiver location, the field strength decreases for higher terrain obstacles and for shorter distances between the obstacle and the receiver location. In this regard, significant attenuation values have been observed for obstacles higher than $\lambda/2$. When the obstacle is located close to the receiver, obstacles lower than $\lambda/2$ can also cause considerable field strength reduction.

The additional field strength loss due to irregular terrain in the MF band follows a positive logarithmic tendency with the obstacle height *h*, and a negative logarithmic tendency with the distance *d,* as shown the equation below.

$$L_{Irr}(dB) = (-17.2 \cdot \log_{10}(d) + 25.1) \cdot (\log_{10}(2.84 \cdot h)) \tag{44}$$

where:

L_{Irr}: loss due to terrain irregularities (dB)

d: distance between the obstacle and the receiver (km)

h: height of the obstacle above the line of sight between transmitter and receiver (in number of wavelengths).

The loss due to terrain irregularities (L_{Irr}) should be subtracted from the field strength value obtained by means of the methods described in previous sections. Values smaller than 1 in the argument of the logarithms should not be considered. For values of d longer than 25 km and obstacle heights h shorter than 2λ, L_{Irr} can be neglected.

If the path profile contains several representative irregularities (compared to wavelength), only the greatest attenuation value due to the most significant obstruction should be considered. This is similar to the approach that many simple multiple-edge diffraction loss computation methods use such as: Epstein-Peterson, Deygout, Bullington, and Giovaneli.

15 Local effects in built-up areas

When a surface wave encounters a built up area, its propagation characteristics are modified by the presence of large structures which are partially electrically conducting or which obstruct the normal propagation. Such structures, great in size but electrically small when compared to the wavelength, cause field strength reductions of significant amplitude in the local surroundings. For planning purposes, local variation occurrences affect the quality of the service and thus may prevent the achievement of satisfactory coverage with good reception, particularly for digital broadcasting services where there is a sharp transition from good quality to the absence of signal. Therefore, the characterization of these local variations is essential for system planners in order to take into account the transmission power increase necessary to overcome different reception impairments.

Measurements in open places, areas, and wide streets within cities have shown that simultaneously with a significant decrease of an average level of a signal (in comparison with a rural district at an identical distance from the transmitter), by approximately 5 dB, the standard deviation of a field is increased. The standard deviations in various areas of a city are not identical – ranging from 1.7 up to 5 dB, on the average $\sigma = 3.5$ dB.

15.1 Measurements into densely built up areas

Measurements of signals from rural transmitters into densely built up urban areas in the court yard of high buildings has shown a sharp decrease of the level of a signal on 15-20 dB; however there are insufficient such cases and statistically significant conclusions cannot be drawn. It is only possible to consider that the standard deviation is at least up to 6-8 dB.

Figures 30 to 33 illustrate the variability of the field strength in built up areas for four frequencies, measured on a route through Moscow and its suburbs. In all cases the signal level in urban areas changes in a chaotic manner. At the lower frequencies the standard deviation of spread in signal level is 3–4 dB. At the higher MF frequencies, in Figures 32 and 33 where the spread of measurements in the built-up area is marked by a dashed line, has a standard deviation of 7-10 dB.

Figure 34 shows similar results obtained in Sao Paulo [60].

The percentage of the distance affected by these local decreases in mobile reception is very dependent on the reception environment, mainly at urban areas. Percentages from 10% (Madrid, Spain) to 18% (Delhi, India) have been observed in urban reception. Percentages for mobile reception in rural areas can be 3% or lower.

The characterization of the urban propagation requires the identification and quantification of the causes that generate long-term and short-term spatial field strength variations. For this purpose, the influence of the distance to the transmitter and the elevation profile features must be eliminated from the analysis.

An extensive analysis has been carried out based on data gathered during four different measurement campaigns for evaluating the DRM (Digital Radio Mondiale) system with mobile reception [61]. Those

measurement campaigns covered the whole range of the MF band (666, 810, 1 060 and 1 260 kHz), and they were carried out in different urban reception environments: Mexico D.F. (Mexico), New Delhi (India) and Madrid (Spain). These cities have quite different urban features and they are representative of noteworthy different kinds of urban environments. In order to perform a representative overall analysis of the urban effects, a total of 96 random routes covering more than 500 km overall were measured and analysed.

FIGURE 30

Field strength variability in built up areas at 171 kHz

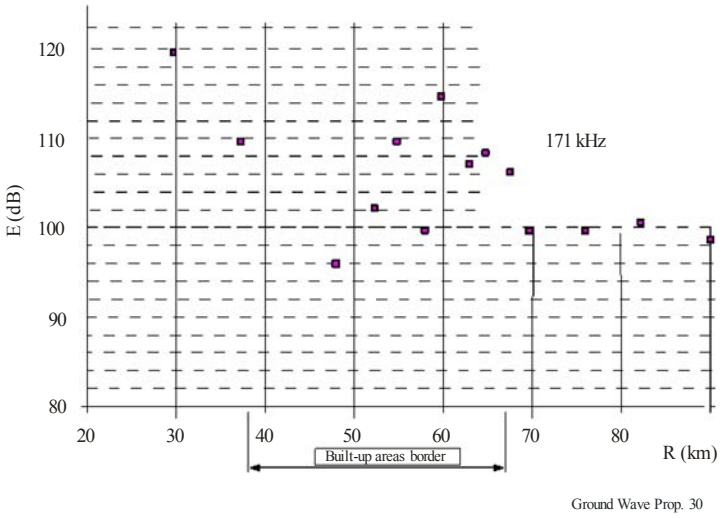

FIGURE 31

Field strength variability in built up areas at 549 kHz

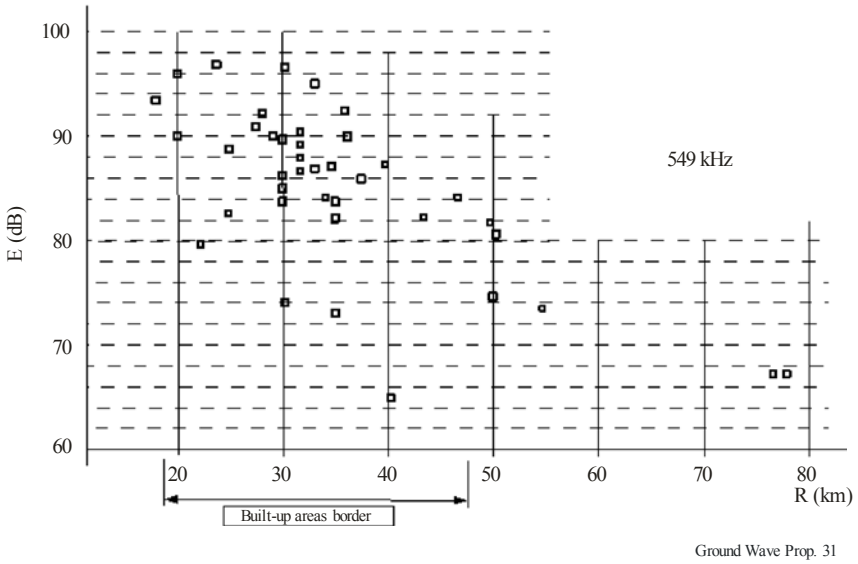

FIGURE 32

Field strength variability in built up areas at 846 kHz

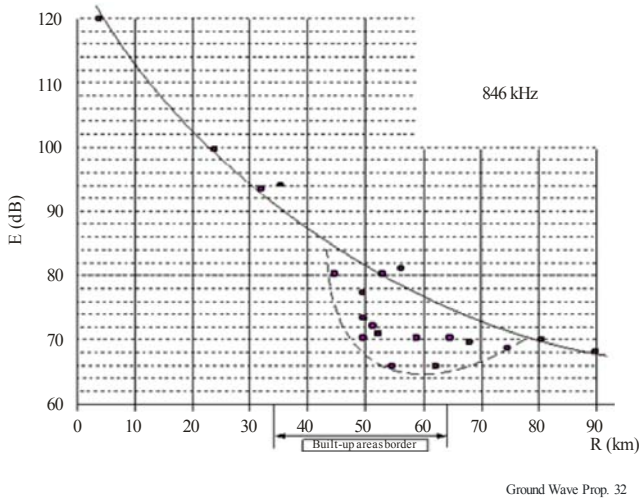

FIGURE 33

Field strength variability in built up areas at 1 359 kHz

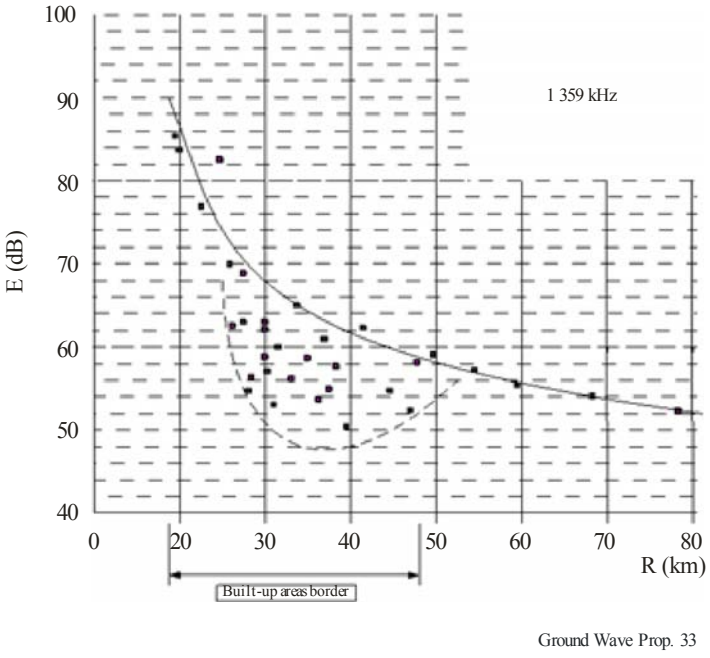

FIGURE 34

Measurements at 1 210 kHz, for 11 routes in Sao Paulo, compared with the prediction from Recommendation ITU-R P.368

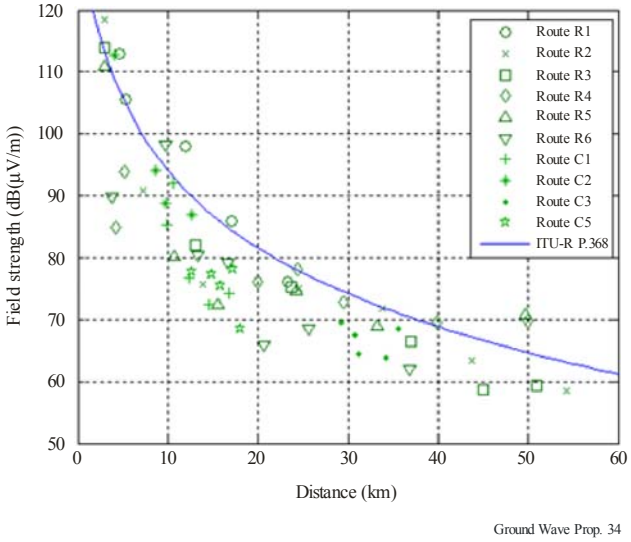

Measurements have also been made at HF [42], Figures 35 to 38. In each case the upper part shows the variation of field strength with distance while, at the bottom of each figure, the standard deviation of the measurements is shown. Unfortunately, in most cases the directional properties of the antenna was not precisely known, and gain corrections have been made on a sector basis.

At short distances between about 100 and 700 m the dependence on distance is close to inverse linear, but between about 700 m and 10 km the dependence is very close to an inverse square-law; approaching the borders of a city (10-24 km from the transmitter) the dependence again becomes flatter.

FIGURE 35

Variation of field strength with distance on approaches to a city, 14 MHz

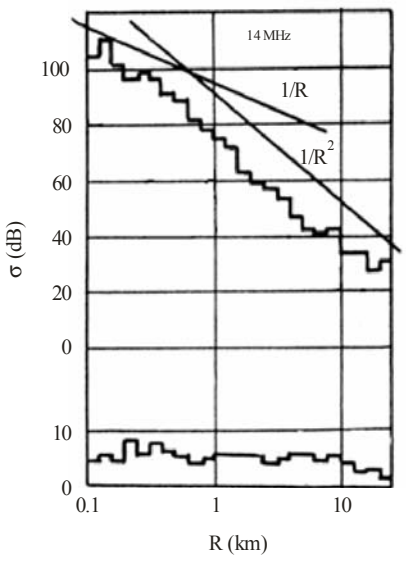

FIGURE 36

Variation of field strength with distance on approaches to a city, 14 MHz

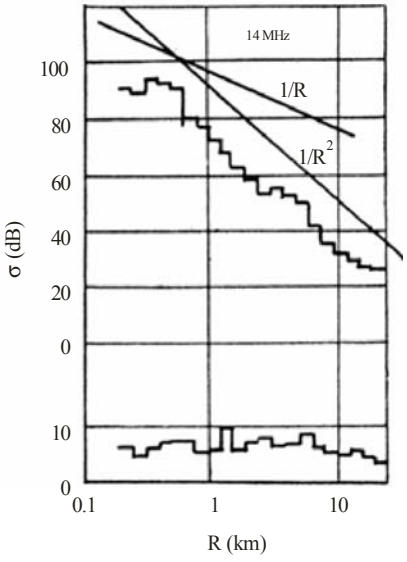

FIGURE 37

Variation of field strength with distance on approaches to a city, 7 MHz

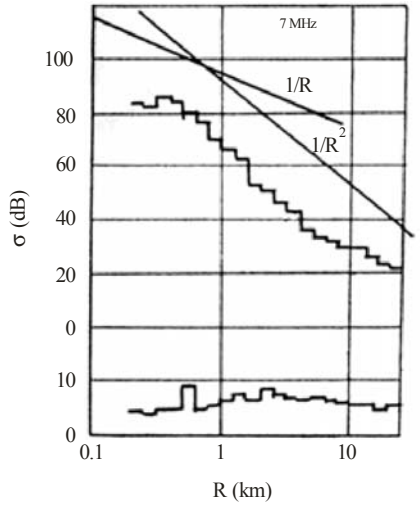

FIGURE 38

Variation of field strength with distance on approaches to a city, 21 MHz

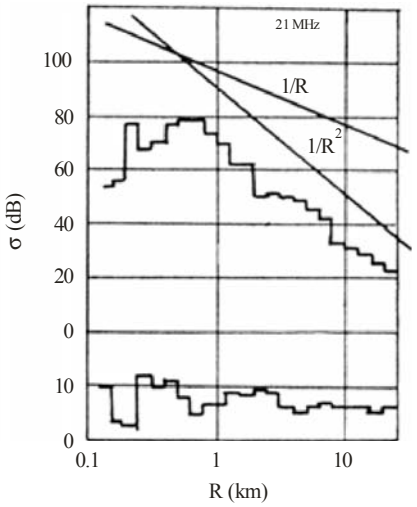

Ground Wave Prop. 37

15.2 Transmission frequency influence in urban environments

Although the importance of the transmission frequency in the field strength variation of broadcasting services in urban reception has been underlined [62], there has been no empirical characterization of this issue. Figures 28 and 30 to 33 show the difference in decibels of the field strength mean values recorded in the same transmission and reception conditions. For example, for two different transmission frequencies (810 kHz and 1 260 kHz), in all cases, field strength values at 810 kHz were higher than those recorded at 1 260 kHz at each reception location.

It has been calculated that the differences are between 6 and 28 dB, most of them between 6 and 16 dB, depending on the specific urban features of the measured areas. The cases where differences are larger than 20 dB values correspond to locations with highest buildings.

15.3 Large scale variation of the field strength

The variations of the spatial long-term component are caused by urban factors that feature dimensions of the same order of magnitude as the optimal value of the averaging window *2L*, given by the Generalized Lee Method. According to results described in a previous section, the averaging window length for urban reception corresponds to the wavelength, in the MF broadcast band ranging from 221 m (1 359 kHz) to 370 m (810 kHz).

The main cause of the large scale variation was found to be the change of the width of streets during signal reception [63], [64]. To quantify the field strength losses due to urban reception, a three-step process was developed. First, results from field trials were classified according to the width of the streets, and mean local values were estimated. Second, mean values of widest streets were compared to propagation curves from Recommendation ITU-R P.368. Last, additional losses due to reception in narrow streets were estimated.

Wide streets with more than eight lanes were chosen as reference in order to quantify long-term variation occurrences. Figure 39 shows the local median values estimated from measurement results in Madrid field trials at 1 260 kHz. As it can be observed, field strength values received in this scenario are close to estimated according propagation curves in Recommendation ITU-R P.368.

FIGURE 39

Local mean field strength median values in wide streets compared to curves from Recommendation ITU-R P.368

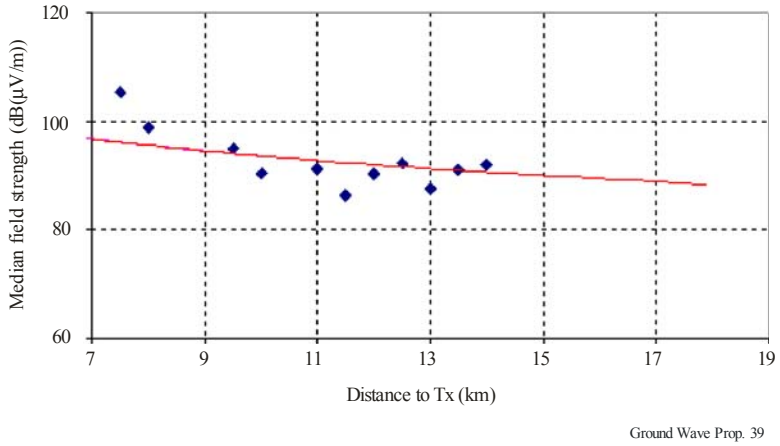

Additional losses in the long-term component due to reception in narrow streets were estimated. Table 4 shows the mean differences between the reference reception scenarios (wide streets containing more than eight lanes) and narrower streets.

The values of additional losses were related to the heterogeneity degree of the urban environment, on the one hand, and to the transmitted frequency, on the other. As it can be observed, Madrid, which shows the most heterogeneous environment, has provided the highest losses values, and at 1 260 kHz the effect is almost double than at 810 kHz.

TABLE 4

Spatial variation at different reception scenarios with respect to curves from Recommendation ITU-R P.368

City – frequency (kHz)	Medium size streets MED ± STD DEV (dB)	Narrow streets MED ± STD DEV (dB)
Delhi – 666	4 ± 1	N/D
Madrid – 810	6 ± 4	12 ± 6
México D.F. – 1060	3 ± 3	9 ± 5
Madrid – 1260	11 ± 6	19 ± 8
Madrid – 1359	N/A	N/A

16 Small scale field strength spatial variation

The presence of power lines, large buildings or metallic construction may increase the field strength in comparison with those in open district by up to 10 dB, or in rare cases reducing it by 15 to 20 dB; it is possible to explain such ambiguity by various variants of the mutual arrangement of the transmitter, metallic constructions and the location of a field measurement.

Table 5 shows empirical median values of occasional fade depth due to the presence of great structures located near the receiver. Measurements were made with a vertical, electric field antenna. The distance over which the field strength variations occur, constitutes spatial fading, i.e. the distance over the mobile reception was affected, seen in a moving vehicle as if it were temporal fading.

TABLE 5

Fade depth and fade length of the field strength variations

Structure	Width (m)	Fade depth (dB)
Highway or road overpass	18-24	23.1
	14-16	12.6
	10-12	9.8
	6-9	8.3
	All	9.1 (mean value)
Pedestrian overpass	2-3	6.5
Sign bridge	-	5.1

17 Indoor propagation

The attenuation of radio signals propagating through and into buildings has an important effect on the performance of radio systems. Frequently, building penetration losses are modelled in order to compute an additional attenuation to the outdoor signal levels. It is also necessary to characterize indoor signal spatial variability in order to quantify the signal variations around its median value.

Indoor radio signal daytime reception at MF has been characterized based on a large database of indoor locations in cities in northern Spain in six different frequencies (612, 639, 990, 1 197, 1 305 and 1 602 kHz) [65]. Indoor measurements in 21 buildings were taken and the total number of locations was 360. In order to quantify the building penetration losses 110 outdoor measurements were also taken along the perimeter of two buildings at every floor.

The field tests have been based on measurements done on existing Amplitude Modulation (AM) commercial transmissions. Nevertheless, the results should be directly applicable to the digital systems since Additive White Gaussian Noise (AWGN) channels have been considered for ground wave propagation in MW at daytime without time and frequency dispersion, so the channel is expected to be flat.

As in many other measurement programs carried out in indoor environments at higher frequency bands, a high spatial variability has been observed even in indoor locations sited few metres apart. Figure 40 shows, as an illustrative example, the median field strength levels obtained in many indoor locations in different buildings as a function of distance at 990 kHz and 1 305 kHz.

FIGURE 40

Median field strength levels in indoor locations at 990 and 1 305 kHz

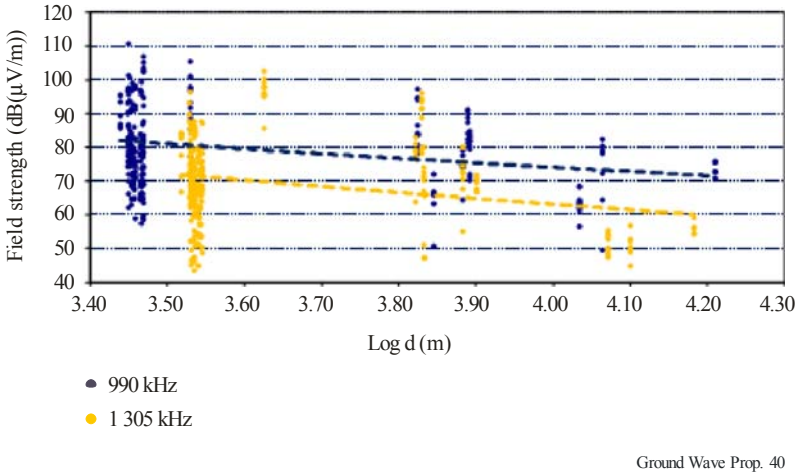

It is seen that the spatial variability is high with differences up to 50 dB between the location with the lowest and highest field strength value within the same building. In fact, it has been observed that indoor median field strength level at MF follows a Log-Normal distribution with a high standard deviation of $\sigma = 11.8$ dB.

It is also observed that the indoor field strength level decreases with distance to transmitter and with the transmission frequency. However, time variability could be ignored, since time standard deviations are smaller than 1 dB.

In order to quantify building penetration losses at MF, the difference between the median field strength value with locations outside the perimeter of a building and the median field strength value with all locations inside the building at the same height has been calculated for every floor in two buildings in northern Spain.

Measurements have also been carried out in Moscow, inside buildings in an entrance and in a lift. These have shown additional signal decreases of up to 8 and 20 dB, and in the metal cabins of lifts up to 40 dB [67].

Since both outdoor and indoor spatial variability are very high, large differences are obtained for building penetration losses for different floors and frequencies, without any clear tendency. Averaging the calculated building penetration losses (every floor and frequency) for the analysed buildings in Madrid, the values 5.9 dB and 7.5 dB are obtained respectively, so a mean value of 6.7 dB is proposed to quantify the building penetration losses at MF.

Indoor signal levels could be predicted by subtracting the building penetration losses from the outdoor predicted field strength values. However, an alternative prediction model is now proposed to be used in order to take as a reference the field strength levels proposed in Recommendation ITU-R P.368 for ground wave propagation in absence of obstacles.

Indoor losses in addition to those given by the ground wave propagation curves in Recommendation ITU-R P.368 have been calculated in each location and linear regressions have been applied to predict indoor losses as a function of frequency in MW [66]:

$$L_{indoor}(dB) = -42.1 + 20.5 \cdot \log(f(kHz)) \tag{45}$$

L_{indoor} losses with respect to the ground wave curves in Recommendation ITU-R P.368 vary from around 15 dB at 600 kHz to 24 dB at 1 600 kHz, calculated from the above prediction formula and are shown graphically in Figure 41.

FIGURE 41

Indoor losses respect to ground wave propagation curves in Recommendation ITU-R P.368

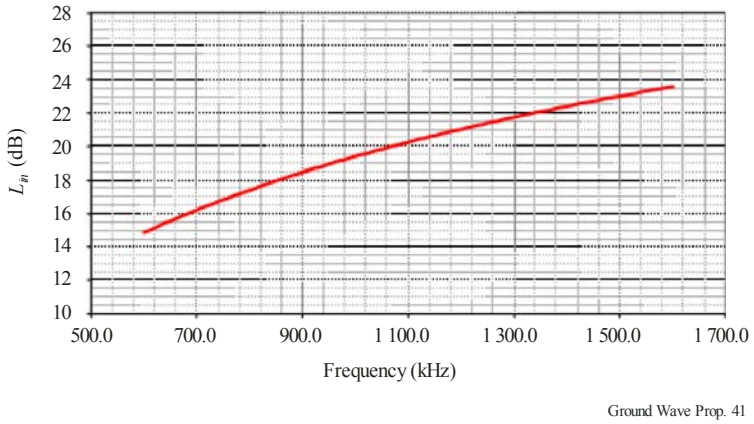

In order to validate the L_{in} prediction equation, it was applied to some indoor DRM signal measurements taken in seven buildings in Madrid and a relatively low mean prediction error of 1.2 dB was obtained.

Consequently, it is recommended to predict the indoor median field strength value exceeded in 50% of locations subtracting the correspondent L_{in} value to the field strength reported in Recommendation ITU-R P.368 as follows:

$$E_{indoor}(dB\mu V/m) = E_{ITU-R\ \ P.368}(dB\mu V/m) + 42.1 - 20.5 \cdot \log(f(kHz)) \quad (46)$$

Then, Log-Normal distribution should be applied with σ = 11.8 dB standard deviation, in order to calculate indoor median field strength levels exceeded in other percentage of locations.

PART 5

18 Measurement methods

18.1 Field strength meter

Field strength measuring techniques are considered in Recommendation ITU-R SM.378. There is a more detailed discussion in the ITU Handbook on Spectrum Monitoring. The Recommendation indicates that an individual measurement will be subject to some uncertainty, with an accuracy of measurement of ±2 dB.

Because measurements of the magnetic field strength are less perturbed in imperfect environments it is preferable to make measurements with a loop antenna (see section 12). Commercial instruments for this purpose will usually be calibrated to convert from magnetic to electric field strength.

An exception to this would be when measurements are made to assess the performance in obstructed environments of receiving systems which use electric field antennas, such as car radios.

Care should be taken to select the best location for the measurement, to represent that environment, as far as possible free from trees, vertical conducting structures and buildings and overhead wires. The small scale variability of the field strength may be countered by making several nearby measurements and selecting the median.

With a portable measuring instrument with a loop antenna, it may be most effective to rotate the loop until a null is found and then to rotate the antenna through 90 degrees to obtain the maximum reading. A peak to minimum ratio of at least 20 dB should be sought, a poorer null will probably indicate a particular problem at that location. In very good locations a ratio of 40 dB may sometimes be achieved.

18.2 Measurement of radiated power

The field may be measured at a distance somewhat beyond the range at which near field effects may be important, at about 1 km from the transmitting antenna. Because of the difficulty of finding good measurement locations in built up areas, a number of measurements should be made and the median value found. If these locations are at different distances from the transmitter, the measurements should be corrected according to the inverse distance field strength relationship. The median measurement should then be compared with the value of 109.5 dB (1μV/m) at 1 km (i.e. 300 mV/m at 1 km) which is the value for 1kW emrp.

In densely built up areas the influence of shadowing from close buildings is rather great. Figure 42 is an example of such measurements at 1 200 kHz, where the transmitting antenna was located between two tall buildings. These measurements have a standard deviation of 6.6 dB [67].

FIGURE 42

Example of measurements close to a transmitter in a densely built up area

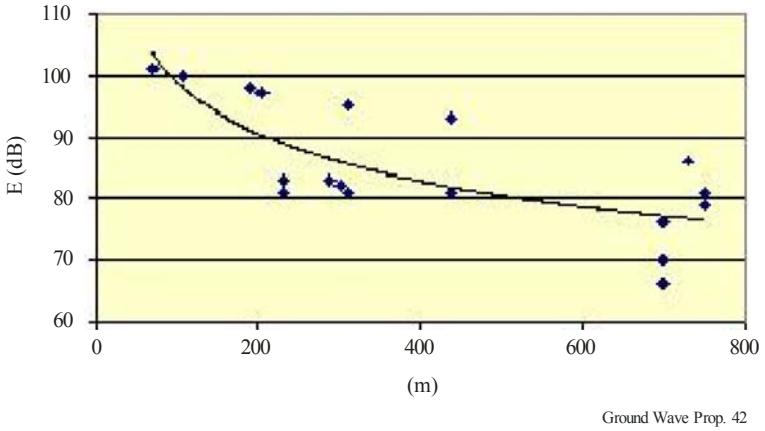

18.3 The measurement of the effective ground conductivity

18.3.1 The attenuation method

Having determined the radiated power, measurements may be made at increasing distances from the transmitter. These measurements should then be normalised to 1 kW emrp, and the trend of results compared with the curves in Recommendation ITU-R P.368 (or from GRWAVE) to find the effective conductivity. If there is a clear discontinuity in the curve, the Millington method could be applied.

Since the measurements will be subject to local variations, and propagation depends on the sub-surface geology, it would be difficult to apply the technique to determine small scale changes in effective conductivity.

DeMinco *et al*. [68] describes a method on how to use the measurements of the Norton Surface Wave propagation between two monopole antennas to determine the ground constants of the soil at the measurement site. Simplified equations for the Norton Surface Wave are contained in the report. The antennas are monopoles mounted on a ground plane where the total antenna assemblies are situated directly on the ground so that only the surface wave is launched. Measurements were performed over the band of frequencies from 30 to 915 MHz at a test site to determine the dielectric permittivity and conductivity.

18.3.2 The reflection coefficient method

In a further report DeMinco [69] describes a method on how to use the measured reflection coefficient and multilayer analysis to determine the ground constants of the multilayer Earth. Measured data is included in both reports. Both reports show equations and graphs for the electric field penetration depth of the soil and its effect on ground-wave propagation.

Also shown in this report is a discussion of the sensitivity of propagation loss to ground conductivity and dielectric constant. As part of the analysis effort, a study was performed using the ITS Undisturbed-Field Model [27] to determine the sensitivity of the propagation loss to variations in conductivity and relative permittivity. The heights of the transmitter and receiver antennas were set equal to zero. The distances used in the analysis and measurements ranged from 2 to 250 metres and covered the frequency range of 30 to 915 MHz. At these short distances and in this frequency range there is still a significant surface wave even at 915 MHz. It was determined that for low conductivity the loss value is very dependent on the value of relative permittivity, but for a higher value of conductivity the loss has less dependence on relative permittivity particularly for frequencies below 150 MHz. The losses also appear to depend on conductivity at frequencies below about 150 MHz. At frequencies above 150 MHz the dependence of propagation loss on conductivity is negligible, but the dependence on relative permittivity is quite significant.

18.3.3 The wave tilt method

The wave-tilt measurement method, which is difficult to apply in practice, depends upon measuring, with a suitably mounted rod antenna, the forward tilt angle, α, of the major axis of the electric field vector and the ratio, a, of the minor to major axis of the ellipse. The method is described by Eaton [70], where he indicates that it requires stringent measurements and very flat uniform terrain.

19 Surface wave phase [71]

19.1 Introduction

The stability of the phase of the surface wave is important for some radionavigation systems.

It is convenient to define the phase of the ground wave, Φ, as the sum of a primary phase and a secondary phase, Φ_S. At a distance, *d,* from a transmitter, the phase of the ground wave may be written:

$$\Phi = nkd + \Phi_s$$

where *n* is the surface value of the refractive index of the atmosphere and $k = 2\pi/\lambda$, where λ is the free-space wavelength. In this equation the secondary phase Φ_S is in units of radians.

However, in most applications it is expressed as a phase delay time in microseconds according to the relationship:

$$t_S = \frac{\Phi_S \ \lambda}{2\pi \cdot 300} = \frac{\Phi_S \cdot 10^6}{2\pi f_{\mathrm{Hz}}}$$

where:

t_s: secondary phase delay time (μs)

Φ_S: secondary phase (rad)

λ: wavelength (m) and

f_{Hz}: frequency (Hz).

19.2 Smooth homogeneous earth

The basic starting point for the calculation of the secondary phase is the theory of ground-wave propagation over a smooth homogeneous earth [72], using methods that are identical to that used to compute the ground-wave amplitude. To extend this basic method to more general cases, it is useful to formulate the calculations in terms of a general surface impedance [73].

19.3 Secondary phase perturbations

At frequencies below about 3 MHz, the smooth homogeneous earth theory can be used to calculate the phase of the ground wave, to the degree of accuracy required for navigation systems, over sea paths including those with large waves. On land paths, however, the secondary phase is modified by changes in the electrical characteristics along the path, terrain irregularities and sub-surface layers [74]. Various methods have been developed for predicting the perturbation in the secondary phase due to these factors [75].

19.4 Non-homogeneous paths

When the electrical characteristics or surface impedance along a path change (e.g. at a land-sea boundary), there is a corresponding sudden change in both the amplitude and phase of the ground wave. The phase in this case can be calculated by the Millington-Pressey method [76]. This method is completely analogous to the Millington method for computing the ground-wave amplitude over non-homogeneous paths. The phase of a ground-wave signal over a two section path can be calculated from the Millington method if the amplitudes in the formulae are replaced with the corresponding homogeneous earth phases.

When the electrical characteristics of the Earth are different in different directions, the wavefront is bent towards the area with the lowest conductivity. This may cause problems for direction finding systems.

19.5 Terrain irregularities

Where there are severe terrain irregularities it is more efficient to use the integral equation method to compute the phase of the ground wave, to give the accuracy desired for navigational applications.

Figure 43 shows a comparison of computational methods and experimental measurement [59]. The path shown crosses both Death Valley, California with an elevation of 100 m below sea level and the Sierra Nevada mountain range. The measured points are shown by the symbol (I). The solid line was calculated by means of the integral equation method. The dotted line was calculated by the Millington-Pressey method with a two-layer smooth earth effective impedance model.

At 100 kHz, a secondary phase of 36 degrees corresponds to 1 μs (see section 19.1 above).

19.6 Meteorological effects

Several investigations of the stability of Loran-C signals have revealed phase variations corresponding to time-of-arrival variations of as much as ± 0.5 μs [77], [78]. These variations have both a diurnal and long-term characteristic and are correlated with changes in the gradient of the dry term of the refractive index of the atmosphere. The longer term variations are associated with the passage of a weather front along the measurement path.

FIGURE 43

A comparison of the measured and calculated phase for the USA West Coast Loran-C system

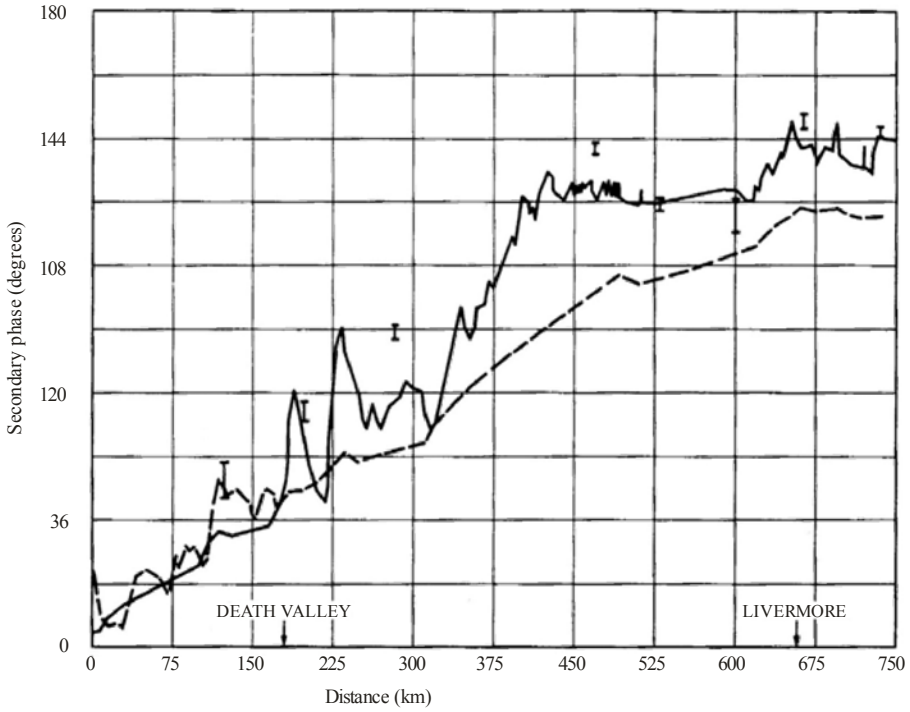

ANNEX 1

The Generalised Lee method

The Lee method [79], [80] is a reference technique to determine the local mean values of the long-term component of the signal variability. A description of this technique is contained in Recommendation ITU-R SM.1708 and also in a CEPT Report [81].

The local mean values are estimated by applying a running mean to a series of instantaneous measurements of field strength, *r(x)*. To do this, it is necessary to determine appropriate values of three different parameters:

– the averaging window $2L$ or distance that should be considered around the point x (the point where the field strength mean value is being calculated);

– the minimum number of independent samples N within each interval $2L$ that are needed to calculate the local mean with a certain level of confidence;

– a minimum distance d between consecutive samples that ensures that samples are uncorrelated.

The local means are assessed by averaging a minimum of N uncorrelated samples, with a distance d between consecutive samples, within an averaging window $2L$.

Lee [79], [80], [82] and later Parsons [83] calculated theoretically the proper values of these parameters for the specific case of a Rayleigh propagation channel and UHF frequency band (with some specific mentions for the VHF band [80]). However, neither the obtained values nor the method to calculate them can be generalized to other reception conditions.

A Generalized Lee Method has been defined [84] to determine the values of such parameters for any reception condition (frequency band, reception environment and propagation factors). This method is summarized in Figure A1.

FIGURE A1

Summary of the Generalized Lee Method

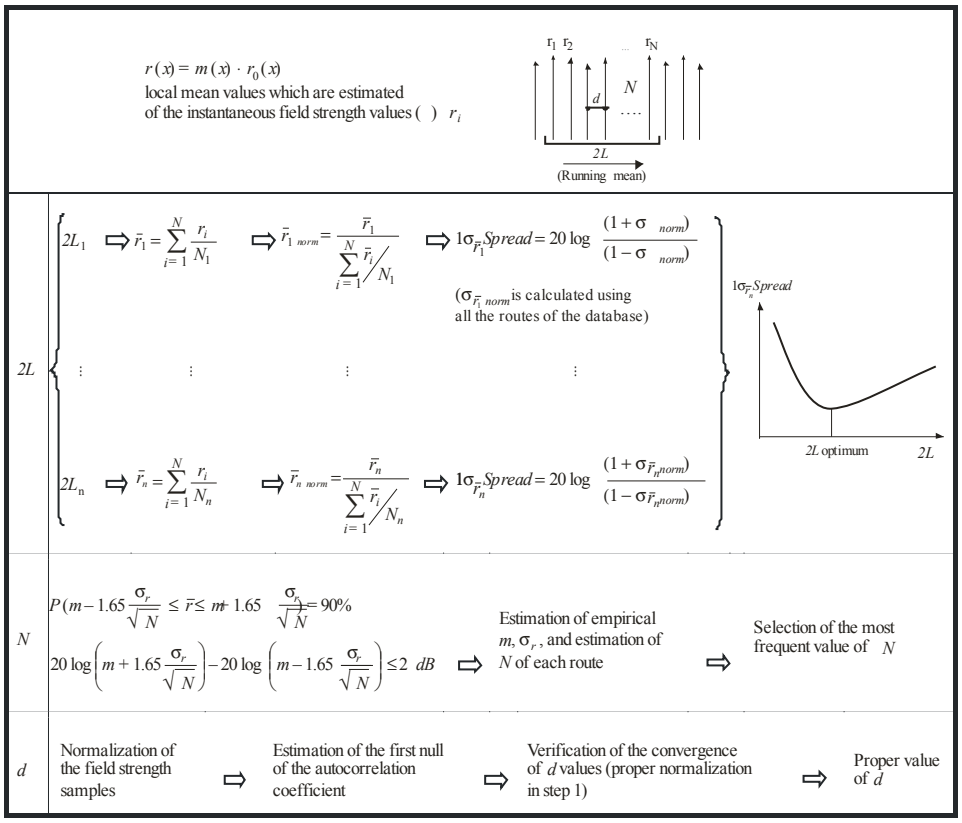

Ground Wave Prop. A1

Values of the method parameters for the MF band

The application of the Generalized Lee Method requires the selection of appropriate values of the above-mentioned parameters (2*L*, *N* and *d*) for the frequency band and reception environment under study. From a set of measurement campaigns [85], [86], values of these parameters were obtained in the case of signals received in the MF band [72], [87], [88], [89]. Table A1 includes a summary of the results obtained for three different types of environment: rural, urban and suburban.

TABLE A1

Reference values of Generalized Lee method parameters for the MF band and different reception environments

Parameter	Reception environment		
	Rural	**Suburban**	**Urban**
2*L*	0.9λ - 2.1λ	0.9λ - 2.1λ	λ
d	0.17λ	0.14λ - 0.16λ	0.05λ
$N^{(1)}$	8	11	20

Note 1 – Values of *N* were obtained for a maximum error from the real mean of 1 dB and a confidence level of 90%.

In all the cases, it is possible to take a minimum number of samples *N* within the averaging window 2*L* fulfilling the requirement for the distance *d* between uncorrelated samples ($N \cdot d \leq 2L$). The use of these values ensures the proper averaging of the field strength local variations.

20 References

[1] Sommerfeld, A.: 'The propagation of waves in wireless telegraphy', *Ann. Phys.,* 1909, 28, p.665.

[2] Norton, K.A.: 'The propagation of radio waves over the surface of the Earth and in the upper atmosphere. Part 1', *Proc. Inst. Radio. Eng.,* 1936, 24. pp. 1367-1387.

[3] Norton, K.A.: 'The propagation of radio waves over the surface of the Earth and in the upper atmosphere. Part 2', *Proc. Inst. Radio. Eng.,* 1937, 25. pp. 1203-1236.

[4] Van Der Pol, B., and Bremmer, H.: 'The diffraction of electromagnetic waves from an electrical point source round a finitely conducting sphere', *Philos. Mag. Ser. 7,* 1937, 24, pp. 141-176 and pp. 825-864; 1938, 25, pp. 817-834; and 1939, 26, pp. 261-275.

[5] Norton, K. A.: 'The calculation of ground-wave field intensity over a finitely conducting spherical Earth', *Proc. Inst. Radio Eng.,* 1941, 29, pp. 623-639.

[6] Millington, G., 1949, 'Ground-wave propagation over an inhomogeneous smooth earth', Proc. IEE, 96, 53.

[7] Hufford, G.A. 1952, "An integral equation approach to the problem of wave propagation over an irregular surface', Quart. Appl. Math, 9, 391.

[8] Ott, R.H., and L.A. Berry, 1970, 'An alternative integral equation for propagation over irregular terrain', Radio Sci., Part 1, 5(5), pp. 767-771.

[9] Hill D.A. "Ground-wave propagation over Forested and Built-up Terrain" NTIA Report 82-114, Dec 1982.

[10] DeMinco, N. "Automated Performance Analysis for Ground-Wave Communication Systems," NTIA-Report 86-209, Dec. 1986.

[11] DeMinco, N "Ground-Wave Analysis Model for MF Broadcast Systems," NTIA-Report 86-203, Sept. 1986.

[12] Kissick, W.A., *et al*., "Measurements of LF and MF Radio Propagation over Irregular, Inhomogeneous Terrain," NTIA-Report 78-12, Nov. 1978.

[13] Hoffman J. R., *et al*., DGPS Field Strength Measurements at a GWEN Site," NTIA-Report 98-346, April 1998.

[14] Ott, R. H. *et al*., "Ground Wave Propagation Over Irregular, Inhomogeneous Terrain: Comparisons of Calculations and Measurements," NTIA Report 79-20, May 1979.

[15] Adams, J. E., *et al*., "Measurements and Predictions of HF Ground Wave Propagation over Irregular, Inhomogeneous Terrain, "NTIA-Report 84-151, July 1984.

[16] DeMinco, N, "Medium Frequency Propagation Prediction Techniques and Antenna Modeling for Intelligent Transportation Systems (ITS) Broadcast Applications," NTIA-Report 99-368, Aug. 1999.

[17] DeMinco, N, "Propagation Prediction Techniques and Antenna Modeling (150 to 1705 kHz) for Intelligent Transportation Systems (ITS), IEEE AP Magazine, AP Vol. 42, No. 4, Aug. 2000, pp. 9-34.

[18] Rotheram, A.S.: 'Ground-wave propagation. Part 1 Theory for short distances', *IEE Proc, F,* 1981,128, pp. 275-284.

[19] Rotheram, A.S.: 'Ground-wave propagation. Part 2 Theory for medium and long distances and reference propagation curves', *IEE Proc. F,* 1918, 128, pp. 285-295.

[20] Rotheram, A.S.: 'Ground-wave propagation', *Marconi Rev.,* 1982, 45, (1), pp. 18-48.

[21] Causebrook, J.H., 1977, 'Groundwave propagation at medium frequency in built-up areas'. BBC Engineering Research Department Report RD 1977/25.

[22] Causebrook, J.H., 1978, 'Medium-wave propagation in built-up areas', Proc. IEE, Vol. 125, 9, pp. 804-808.

[23] Bremmer, H.: Terrestrial Radio Waves' Elsevier, 1949.

[24] Picquenard, A. “Radio Wave Propagation”, New York: John Wiley and Sons, 1974, p. 80.

[25] Craig K.H. “Clear Air Characteristics of the Troposphere”, in “Propagation of radio waves” 2nd ed, ed Barclay L W, 2003 ISBN 0 85296 102 2, Chapter 7.

[26] “Ground wave propagation in an exponential atmosphere”, CCIR Report 714-2, 1990.

[27] DeMinco, N “Propagation Loss Prediction Considerations for Close-In Distances and Low Antenna Height Applications,” NTIA-Report TR-07-449, July 2007.

[28] Кашпровский В.Е., Кузубов Ф.А., "Распространение средних радиоволн земным лучом" (Kashprovsky V.E., Kuzubov F.A., "Propagation of medium waves by terrestrial ray"), "Svyaz", 1971, 220 pages.

[29] Feinberg, E.L., “Propagation of radiowaves along a terrestrial surface” Iss AS USSR M 1961, p.546.

[30] Millington G, 1949, Nature 163 p. 128.

[31] Millington G. and Isted G.A. 1950 “Ground-wave propagation over an inhomogeneous Earth, Part 2 Experimental evidence and practical implications”, Proc. IEE, 97, 209.

[32] Hoffman, J.R., *et al*., “Field Strength Measurements of DGPS and FAA Beacons in the 285 to 315 kHz Band,” NTIA-Report 97-337, June 1997.

[33] Damboldt Th. 1981 “HF ground-wave field strength measurements on mixed land-sea paths”, IEE 2nd Int Conf Antennas and Propagation, Heslington, York, UK; IEE Conf Proc No. 195.

[34] Barrick, D.E., (1971a), "Theory of HF and VHF propagation across the rough sea, 1, The Effective Surface Impedance For A Slightly Rough Highly Conducting Medium At Grazing Incidence", Rad. Sci, V6, pp 517-526.

[35] Barrick, D.E., (197Ib), "2. Application to HF and VHF propagation over the sea", Rad. Sci., V6 pp 527-533.

[36] Phillips, O.M. (1957): “On the generation of surface waves by turbulent wind”, J. Fluid Mech., Vol.2, pp. 417-445.

[37] Furutsu, K. Radio Science vol 17 pp 1037-1050, 1982.

[38] J.M. Pielou, J.D. Milsom and R N Herring “HF ground wave propagation from a cliff top site” IEE Conf ICAP87, p103, 1987

[39] Chernov Yu. A., Zhiltsov A.U. “The Statistical characteristics of a terrestrial wave in a range LF-MF”, “Radiotekhnika”, 1997, № 2, PP. 41-45.

[40] Stratton G.A., “The Theory of electromagnetism”, “Gostekhizdat”, 1948.

[41] Chernov Yu. A. “Distribution of average radiowaves in urban environment”, Trudy NIIR, 2004, PP. 131-136.

[42] Buchatskaja G.B. “An experimental research of distribution of a field HF-waves in city for a transmitter, located within the limits of this city”, Trudy NIIR, 1989, № 4, PP. 14-19.

[43] Bown, R. Martin, D.K. and Potter, R.K. “Some Studies in Radio Broadcast Transmission” 1924, Proc IRE V12 pp. 57-131.

[44] Bown, R and Gillett, G.D., “Distribution of radio Waves From Broadcasting Stations Over City Districts” 1924, Proc IRE V12 pp. 395-409.

[45] Barfield, R.H. and Munro, G.H. “The Attenuation of Wireless waves Over Towns”, 1929, Proc IEE, V67, pp. 253-270.

[45] Naismith, R. “Field Strength Measurements on Daventry 5XX”, 1931, Proc IEE V69 pp. 881-890.

[47] Causebrook, J.H “Medium-wave propagation in built-up areas”, 1978, Proc. IEE, V125, pp. 804-808.

[48] Luo Lichen, “A New MF and HF Ground-wave Model for Urban Areas”, 2000, IEEE Antennas and Prop. Mag, V42, pp. 21-32.

[49] Gracely, F.R. “ Temperature Variations of Ground-Wave Signal Intensity at Standard Broadcast Frequencies ”, Proc. I.R.E., April, 1949, pp. 360-363.

[50] Gerber W. and A. Werthmüller, Ueber die vegetabile Absorption der Bodenwelle, Techn. Mitt.T.T., Sw., 1945, №1, 12-19.

[51] Chernov Yu. A. "Seasonal changes of a field intensity of a ground wave in day time in LF and MF bands" Trudy NIIR, 2005, pp. 109-115.

[52] Захаренко В.Н.,"Влияние вариаций электропроводности подстилающей поверхности на амплитуду напряженности земной волны диапазонов СВ и ДВ", Электросвязь, 1992, №1, pp. 34-35. [V.N. Zakharenko, "Influence of variations in electroconductivity of a ground surface on amplitude of intensity of a ground wave signal in the MF and LF bands", Elektrosvyaz, 1992, №1, pp. 34-35.

[53] Recommendation ITU-R P.1321-3.

[54] Чернов, Ю.А, Цифровое радиовещание до 30 МГц: иллюзии и реальность. *Часть 2.* Длинные и средние волны. Темное время суток, Электросвязь, 2012, №2. (Yu. Chernov, Digital broadcasting up to 30 MHz: illusions and reality. Part 2. LW and MW. Dark time of day, Electrosvyaz, 2012, № 2.).

[55] Causebrook J H and Tait B, 1979, "Ground Wave propagation in a realistic terrain" BBC Research Dept Report RD 1979/19.

[56] ERC Recommendation (00)08, 2000, "Field Strength Measurements along a Route with Geographical Coordinate Registrations" http://www.erodocdb.dk/docs/doc98/Official/Pdf/Rec0008.pdf.

[57] Ott, R.H. 1971, 'An alternative integral equation for propagation over irregular terrain', Radio Sci., Part 2, 6(4), pp. 429-435.

[58] de la Vega, D *et al*., "Analysis of the Attenuation Caused by Orography Influence in the Medium Wave Band", 2007 IEEE 65th Vehicular Technology Conference - VTC2007.

[59] Wait J R 1962, "Electromagnetic Waves in Stratified Media," Oxford, Pergamon.

[60] Almeida, M.P.C. ; David, R.P.; Souza, R.S.L.; Castellanos, P.V.G. ; Cal Braz, J.A.; Lima, M.V.; Lima, F.F.; Silva Mello, L.A.R.; "Medium wave DRM field trials in Brazil - some daytime and night-time results in urban environment", Measurement (London. Print), v. 45, p. 1-9, 2012.

[61] Report ITU-R BS.2144. "Planning parameters and coverage for Digital Radio Mondiale (DRM) broadcasting at frequencies below 30 MHz", May 2009.

[62] Causebrook, J.H., 1977, "Ground Wave Propagation at Medium Frequency in Built-up Areas" BBC Research Dept Report 1977/25.

[63] Gil, U, *et al*., 2009, "Medium Wave Field Strength Spatial Variability in Urban Environments", 3rd European Conference on Antenas and Propagation 2009.

[64] Gil, U, *et al*., 2010, "Empirical Analysis of Medium Wave Field Strength Prediction in Urban Environments", IEEE Int Symposium on Broadband Multimedia Systems and Broadcasting. Shanghai 2010.

[65] Fernandez, I, *et al*., 2011, Carrier and Noise Measurements in the Medium Wave Band for Urban Indoor Reception of Digital Radio" IEEE Trans Broadcasting.

[66] Fernandez, I, *et al*., 2011, Carrier and Noise Measurements in the Medium Wave Band for Urban Indoor Reception of Digital Radio" IEEE Trans Broadcasting.

[67] Chernov Yu, "Distribution of terrestrial wave signal levels in a service zone at medium frequencies" Trans NIIR, 2006, pp. 81-90.

[68] DeMinco, N., *et al*., "Free-Field Measurements of the Electrical Properties of Soil Using the Surface Wave Propagation Between Two Monopole Antennas," NTIA-Report TR-12-484, January 2012.

[69] DeMinco,, N., *et al*., "Free-Field Measurements of the Electrical Properties of Soil Using the Measured Reflection Coefficient at Normal Incidence and Multilayer Analysis," NTIA-Report TR-13-494, February 2013.

[70] Eaton J L 1976 "The wave tilt method of measuring electrical ground constants in the lf and mf bands" BBC Research Report RD 1976/15. www.bbc.co.uk/rd/pubs/reports/1976-15.pdf.

[71] CCIR Report 716-3, 1990.

[72] Johler, J.R., Kellar, W.J. and Walters, L. C. 1956, "Phase of the low radio-frequency ground wave". NBS Circular 573, http://tf.boulder.nist.gov/general/pdf/2302.pdf.

[73] Hill, D.A. and Wait, J. R., 1980, 2Ground-wave attenuation function for a spherical earth with arbitrary surface impedance". *Radio Sci.* Vol. 15, 3.

[74] Johler, J.R. and Horowitz, S. 1974 "Propagation of a Loran pulse over irregular, inhomogeneous ground". Paper 28, AGARD Conf. Proc. No. 144 on Electromagnetic wave propagation involving irregular surfaces and inhomogeneous media, ed A. N. Ince. NTIS Accession Number AD A008583, National Technical Information Service, Springfield, Va. 22161, USA.

[75] Samaddar, S.N. 1979, "The theory of Loran-C ground-wave propagation - A review". *Navigation,* Vol. 26, 3.

[76] Pressey, B.G., Ashwell, G.E. and Fowler, C.S. 1953, "The measurements of the phase velocity of ground-wave propagation at low frequencies over a land path". *Proc. 1EE,* 100, Pt. III.

[77] Doherty, R.H. and Johler, J. R. 1975, " Meteorological influences on Loran-C ground-wave propagation". *J. Atmos. Terr. Phys.,* Vol. 37, pp. 1117-1124.

[78] Samaddar, S. N. 1980 "Weather effects on Loran-C propagation". *Navigation,* Vol. 27, 1.

[79] Lee, W C Y, 1986, "Mobile Communications Design Fundamentals", Howard W. Sams and Co.

[80] Lee, W C Y, 1985, "Estimate of Local Average Power of a Mobile Radio Signal", IEEE Trans Vehicular Technology, Vol. VT-34, Nº 1.

[81] "ERC Recommendation (00)08, 2000, "Field Strength Measurements along a Route with Geographical Coordinate Registrations" http://www.erodocdb.dk/docs/doc98/Official/Pdf/Rec0008.pdf.

[82] Lee, W C Y, 1982, "Mobile Communications Engineering", Ed. McGraw-Hill Book Company.

[83] J. D. Parsons, 2000, "The Mobile Radio Propagation Channel", 2nd. Ed, John Wiley & Sons Ltd, 2000, ISBN 0 471 98857 X.

[84] de la Vega, D, *et al*., 2009 "Generalization of the Lee Method for the Analysis of Signal Variability", IEEE Trans Vehicular Technology, Vol. 58, Nº 2, pp. 506-516.

[85] Gil, U, et al. 2008, "DRM Field Trials for Urban Coverage in Spain", EBU Technical Review 2008-Q2.

[86] Gil, U, et al.2008, "DRM 20 kHz Simulcast Field Trials in the Medium Wave Band in Mexico D.F." IEEE Trans Broadcasting, Vol. 54, Nº 1, pp. 58-61.

[87] de la Vega, D, *et al*., 2008, "Evaluation of the Lee Method for the Analysis of the Long-Term and Short-Term Variations in the Digital Broadcasting Services in the MW Band", IEEE Int Symposium on Broadband Multimedia Systems and Broadcasting, Las Vegas, USA, March 2008.

[88] de la Vega, D, *et al*., 2008, "Empirical Analysis of the Sample Correlation for the Planning of Field Trials in the Digital Broadcasting Services at MF Band," Proc IEEE Int Instrumentation and Measurement Technology Conference - I2MTC 2008, pp. 2201-2204, Victoria BC, Canada, May 2008.

[89] Gil, U, *et al*., 2010, "Statistical Characterization of the Medium Wave Field Strength Spatial Variability in Urban Environments Using the Generalized Lee Method" Proc. 4th European Conf on Antennas and Propagation, Barcelona, Spain, April 2010.

International Telecommunication Union
Sales and Marketing Division
Place des Nations
CH-1211 Geneva 20
Switzerland
Fax: +41 22 730 5194
Tel.: +41 22 730 6141
E-mail: sales@itu.int
Web: www.itu.int/publications

Printed in Switzerland
Geneva, 2014